

**NONLINEAR ESTIMATION OF WATER NETWORK DEMANDS  
FROM LIMITED MEASUREMENT INFORMATION**

A Thesis

by

AHMED IBRAHIM ELSAID RABIE

Submitted to the Office of Graduate Studies of  
Texas A&M University  
in partial fulfillment of the requirements for the degree of

MASTER OF SCIENCE

December 2008

Major Subject: Chemical Engineering

**NONLINEAR ESTIMATION OF WATER NETWORK DEMANDS  
FROM LIMITED MEASUREMENT INFORMATION**

A Thesis

by

AHMED IBRAHIM ELSAID RABIE

Submitted to the Office of Graduate Studies of  
Texas A&M University  
in partial fulfillment of the requirements for the degree of

MASTER OF SCIENCE

Approved by:

Chair of Committee,  
Committee Members,

Head of Department,

Carl Laird  
Mahmoud El-Halwagi  
Juergen Hahn  
Guy L. Curry  
Michael Pishko

December 2008

Major Subject: Chemical Engineering

## ABSTRACT

Nonlinear Estimation of Water Network Demands from  
Limited Measurement Information. (December 2008)

Ahmed Ibrahim Elsaied Rabie, B.Sc., Cairo University; M.Sc., Cairo University

Chair of Advisory Committee: Dr. Carl Laird

Access to clean drinking water is very important to the health and well-being of the population. Mathematical modeling, optimization, and online estimation are needed to solve challenging problems in water network applications such as the requirement to meet the new dynamic regulations in the Safe Drinking Water Act and the Clean Water Act. This includes providing sufficient capacity to satisfy uncertain and changing water demands, maintaining consistent water quality, and identifying and responding to abnormal events. In most of these applications, reliable knowledge of the water flow velocity is necessary. However, in practice, few measurements are usually available. This work uses a nonlinear optimization framework to estimate the unknown water demands and velocities from limited measurements. The problem is formulated as a constrained nonlinear least squares estimation problem. The constraints represent the basic governing mass and energy conservation laws as well as some operational constraints. Given the limited number of flow measurements, the estimation problem is ill-posed. Non-unique solutions may exist in which many demand profiles can match the limited number of measurements. Offline estimates of the demand patterns based on historical data are used to regularize the problem and force a unique solution. In the first phase of this project, a hydraulic model was developed for water distribution systems. This model showed very good agreement when it was validated against the simulator EPANET using 3 case studies. In the second phase, the estimation formulation was tested using the same 3 case studies with different sensor configurations. In each of the case studies, estimation results are reasonable with fewer sensors than the available degrees of freedom.

## ACKNOWLEDGEMENTS

All thanks and praises are due to ALLAH who gave me the ability to complete the work of this research.

I would like also to thank my advisor and the committee chair, Dr. Carl Laird who was so patient with me. Dr. Laird has supported me from the first working day and provided me with excellent academic assistance.

I would like also to thank Prof. Mahmoud El-Halwagi for his continuous support and his continuous encouragement. I would like also to thank my committee members, Dr. Juergen Hahn and Prof. Guy Curry for their guidance throughout the course of this thesis.

Thanks also go to my friends and colleagues and the department faculty and staff for making my time at Texas A&M University a great experience. Finally, great thanks to my father and my mother for their encouragement and to my wife for her patience and love.

## TABLE OF CONTENTS

	Page
ABSTRACT .....	iii
ACKNOWLEDGEMENTS .....	iv
TABLE OF CONTENTS .....	v
LIST OF FIGURES .....	vii
LIST OF TABLES .....	x
 CHAPTER	
I INTRODUCTION .....	1
II LITERATURE REVIEW .....	3
III HYDRAULIC MODELING IN WATER NETWORKS .....	7
3.1 Modeling Fundamentals and Assumptions .....	8
3.1.1 Mechanical Energy Balance .....	10
3.1.2 Hydraulic Grade Lines .....	11
3.2 Distribution System Component Models .....	13
3.2.1 Nodes .....	13
3.2.1 Links .....	16
IV PROBLEM DEFINITION AND MATHEMATICAL FORMULATION ..	24
4.1 Problem Definition .....	24
4.2 Problem Formulation .....	25
4.3 Challenges .....	27
4.3.1 Discretization for the ODE in Tanks .....	27
4.3.2 Unknown Flow Direction .....	28
4.3.3 Pump Switching and Tank Level Control .....	29
4.4 Validation of the Optimization Model .....	30

CHAPTER	Page
V	MODEL VALIDATION ..... 32
5.1	Validation Formulation ..... 32
5.2	Case Studies ..... 33
5.2.1	Case Study 1 ..... 33
5.2.2	Case Study 2 ..... 35
5.2.3	Case Study 3 ..... 37
5.3	Validation Results ..... 39
5.3.1	Validation Results for Case Study 1 ..... 39
5.3.2	Validation Results for Case Study 2 ..... 46
5.3.3	Validation Results for Case Study 3 ..... 50
VI	RESULTS AND DISCUSSION ..... 54
6.1	Selecting Flow Measurements ..... 55
6.1.1	Fundamentals of Graph Theory ..... 56
6.1.2	Chord Flow Decomposition Method ..... 59
6.2	Case Studies ..... 62
6.2.1	Case Study 1 ..... 63
6.2.2	Case Study 2 ..... 67
6.2.3	Case Study 3 ..... 70
VII	CONCLUSION AND RECOMMENDATIONS ..... 75
7.1	Summary ..... 75
7.2	Conclusion ..... 75
7.3	Recommendations ..... 76
	REFERENCES..... 77
	APPENDIX A ..... 82
	VITA ..... 94

## LIST OF FIGURES

		Page
Figure 3-1:	Schematic Diagram for a Water Network Distribution System.....	9
Figure 3-2:	Schematic Diagram Showing the Energy Grade Line (EGL) and the Hydraulic Grade Line (HGL), (Walski et al. 2001). .....	12
Figure 3-3:	Pump Head-Discharge Curve, (Walski et al. 2001).....	20
Figure 3-4:	Schematic Diagram for the Nodal Demand Daily Distribution, (Walski et al. 2001) .....	23
Figure 4-1:	Adjusting the Flow Direction in the Model.....	28
Figure 4-2:	A Schematic Diagram for the Validation Problem.....	31
Figure 5-1:	A Schematic Diagram for Case Study 1 .....	33
Figure 5-2:	Demand Pattern in Case Study 1 .....	35
Figure 5-3:	Layout of Case Study 2.....	36
Figure 5-4:	A Schematic Diagram for Case Study 3 .....	37
Figure 5-5:	Normalized Flow in Links (12, 31, 121, and 122) in Case Study 1 .....	43
Figure 5-6:	Normalized Flow in Links (11, 21, 111, and 112) in Case Study 1 .....	43
Figure 5-7:	Normalized Head at Nodes (10, 11, 23, and 32) in Case Study 1 .....	44
Figure 5-8:	Normalized Head at Nodes (12, 21, 22, and 31) in Case Study 1 .....	44
Figure 5-9:	Normalized Head in Tank (2) in Case Study 1 .....	45
Figure 5-10:	Normalized Flow in Links (2, 11, 17, and 37) in Case Study 2 .....	48
Figure 5-11:	Normalized Flow in Links (1, 25, and 31) in Case Study 2.....	48
Figure 5-12:	Normalized Head at Nodes (1, and 7) in Case Study 2.....	49

	Page
Figure 5-13: Normalized Head at Nodes (14, 19, 21, and 27) in Case Study 2.....	49
Figure 5-14: Normalized Level in Tank (26) in Case Study 2.....	50
Figure 5-15: Normalized Flow in Links (251, and 277) in Case Study 3.....	51
Figure 5-16: Normalized Flow in Links (111, 171, and 241) in Case Study 3 .....	51
Figure 5-17: Normalized Head at Nodes (101, 121, and 145) in Case Study 3.....	52
Figure 5-18: Normalized Head at Nodes (179, 157, and 265) in Case Study 3.....	52
Figure 5-19: Normalized Head at Nodes (199, 219, and 237) in Case Study 3.....	53
Figure 5-20: Normalized Level in Tanks (1, 2, and 3) in Case Study 3 .....	53
Figure 6-1: A Schematic Diagram for the Real Problem.....	54
Figure 6-2: (a) Directed Cyclic; (b) Undirected Acyclic; (c) Undirected Connected; (d) Directed Disconnected Graph .....	56
Figure 6-3: All Possible Trees on a Graph with Six Nodes.(Bondy and Munty 1967) .....	57
Figure 6-4: Illustrative Example Network .....	60
Figure 6-5: Pseudo Demand Links, Branches, and Chords in the Example Network.....	61
Figure 6-6: Chord and Tree Links and Sequence of Adding Measurements in Case Study 1, Configuration 1 .....	63
Figure 6-7: % Error in Flow in Network1 with 0.1 Standard of Deviation in the Offline Demand Function .....	64
Figure 6-8: % Error in Flow in Case Study 1 with Different Standards of Deviation in the Offline Demand Function .....	65
Figure 6-9: Chord and Tree Links and Sequence of Adding Measurements in Case Study 1, Configuration 2.....	66
Figure 6-10: % Error in Flow in Case Study 1 for Two Measurements Configuration.....	66



	Page
Figure 6-11: A Schematic Diagram for Case Study 2 .....	67
Figure 6-12: Planar Graph for Case Study 2 with One Possible Configuration for the Chord and the Tree Links.....	68
Figure 6-13: % Error in Flow in Case Study 2 with 0.1 Standard of Deviation in the Offline Demand Function .....	69
Figure 6-14: % Error in Flow in Case Study 2 with Different Standards of Deviation in the Offline Demand Function .....	70
Figure 6-15: A Schematic Diagram for Case Study 3 .....	71
Figure 6-16: The Depth-First Search and the Resulting Tree for the Network Show in Figure 6-3.....	72
Figure 6-17: The Breadth-First Search and the Resulting Tree for the Network Shown in Figure 6-3 .....	73
Figure 6-18: % Error in Flow in Case Study 3 with 0.1 Standard of Deviation in the Offline Demand Function .....	74
Figure 6-19: % Error in Flow in Case Study 3 with Different Standards of Deviation in the Offline Demand Function .....	74

## LIST OF TABLES

		Page
Table 3-1:	Hazen-William Roughness Coefficient for Different Pipe Materials, (Rossman 2000) .....	18
Table 4-1:	Degrees of Freedom Analysis for Hydraulic Calculations in Water Networks ...	30
Table 5-1:	Input Data for Nodes in Case Study 1 .....	34
Table 5-2:	Input Data for Links in Case Study 1 .....	34
Table 5-3:	Input Data for Selected Nodes in Case Study 2 .....	36
Table 5-4:	Input Data for Selected Links in Case Study 2 .....	36
Table 5-5:	Input Data for Selected Nodes in Case Study 3 .....	38
Table 5-6:	Input Data for Selected Links in Case Study 3 .....	39
Table 5-7:	Water Flow Rates in Link (10) in Case Study 1 .....	40
Table 5-8:	Normalized Flow in Link (112) in Case Study 1 .....	41
Table 5-9:	Normalized Flow in Link (31) in Case Study 1 .....	41
Table 5-10:	Normalized Head at Node (20) in Case Study 2 .....	46
Table 5-11:	Normalized Flow in Link (11) .....	47
Table 5-12:	Normalized Flow in Link (17) .....	47

## CHAPTER I

### INTRODUCTION

Availability of clean drinking water is vital to the health and well-being of the population. Drinking water is usually delivered from treatment facilities to consumers through large storage and piping networks known as the water distribution systems. There are number of challenges that face the successful operation of these water networks. For instance, new regulations in the Safe Drinking Water Act and the Clean Water Act should be met. In addition, many utilities also face changing state legislation. Utilities are required to ensure sufficient capacity to satisfy uncertain and changing water demands, maintain consistent water Quality, identify and respond to abnormal events, improve efficiency through reduced energy usage, and ensure long-term sustainability and reliability of the aging system. Computational modeling, optimization, and online estimation are essential tools to help meet these challenges.

Many water network applications such as disinfectant control, fault detection, and identification strategies require knowledge about the network flow velocities in the system. However, in reality, very few real-time measurements are typically available from the system. Therefore, there is a need to develop an online strategy that can provide reliable estimates of the network demands that can then be used to determine the network flow rates.

This work addresses this concern and demonstrates that nonlinear programming can be used to estimate the unknown water demands and water flows. The water distribution system can be modeled with a large set of differential-algebraic equations and the estimation problem is formulated as a constrained nonlinear least squares problem.

---

This thesis follows the style of *Journal of Water Resources Planning and Management*.

The constraints are those governing equations in the mathematical model that describe basic mass and energy conservation laws as well as some operational constraints. Given the limited number of flow measurements, the estimation problem is ill-posed. Non-unique solutions may exist in which many demand profiles can match the limited number of measurements. This research exploits the availability of offline estimates of the demand patterns which regularizes the problem and forces a unique solution.

The structure of the thesis will be as follows: Chapter II gives an overall literature review on water network modeling, operation, and monitoring. Chapter III introduces the basic concepts in hydraulic modeling and gives detailed description of the water network infrastructure and its basic components. The governing conservation laws in general form are also discussed. Chapter IV presents the problem formulation, outlines the challenges and addresses these challenges.

In chapter V, the model is validated against the water software package EPANET using three different case studies. Chapter VI demonstrates the effectiveness of the estimation formulation for different sensor configurations. Appropriate allocation of sensors is completed using a graph theory approach. The estimation is tested using the same three case studies, with increasing demand noises. Chapter VII summarizes the main results, gives conclusions, and suggests some recommendations for future work.

## **CHAPTER II**

### **LITERATURE REVIEW**

Early studies concerned with hydraulic modeling in water networks involved a formulation and solution strategy for the energy, continuity and friction losses equations. Since this time, solution methods have been improved considerably enabling simulation of large water distribution systems (Wood and Funk 1993). The development of these models along with similar contributions in water modeling have facilitated further research in other related areas such as optimal design and operation of water networks (Goulter 1992).

The classic optimal design problem for water distribution systems seeks to determine the pipe diameters that minimize the total capital cost of the network while satisfying hydraulic and operational constraints. Operational constraints include specified water consumption rates (demands) or minimum pressure at the nodes (Eiger et al. 1994).

Solution methodologies of this problem started with traditional methods utilizing some basic “rules of thumb” and “trial and error” techniques. Poor solution quality and efficiency limited the extension of such methods (Vairavamoorthy and Ali 2000). On the contrary, different optimization techniques have been developed and improved the ability to obtain global or near to global solution in reasonable time. These techniques included linear programming (Alperovits and Shamir 1977; Quindry et al. 1981), nonlinear programming (Morgan and Goulter 1985, Varma et al. 1997), Genetic algorithms (Savic and Walters 1997; Vairavamoorthy and Ali 2000). Further research intended to either improve the solution quality (Fujiwara and De Silva 1990), consider reliability (Fujiwara and Tung 1991; Kapelan et al. 2005), and include water sources of different qualities (Ostfeld and Salomons 2004).

Optimal operation of water networks also has been gaining increasing attention in the last two decades. The inability to meet the pressure requirement at one node or more in the system can

affect the quantity of the received supply (demand), while inability to control the water quality can result in water contamination that damage the public health (Kizilenis 2006).

On the water quality side, research has focused on maintaining water quality within a certain standard threshold concentration by the injection of commercial disinfectant such as chlorine. The motivation was to commit with the regulations issued by the Environmental Protection Agency (EPA) under the U.S Safe Water Drinking Act of 1974 and its amendments in 1986 (SWDAA), which require a minimum chlorine residual 0.2 mg/l to be present at the points of water consumption (Zierolf et al.1998). This commitment increased after the new regulations issued by (EPA) in 1990 which require water quality specifications to be met at the consumers' taps rather than the source treatment plants (Kizilenis 2006).

Chlorine is injected at one or more of the water sources to control the growth of the microorganisms or other types of contaminations. As chlorine travels, it reacts with different types of materials in the bulk phase of water and with the pipe wall as well. Long residence times and low flow velocities cause excessive decay in chlorine concentration. Thus, the source concentration must be large enough to maintain adequate residual chlorine concentration at the consumption nodes. However, high chlorine concentration leads to unpleasant taste and odor. Additionally, studies showed that chlorine and chlorine by-products with high concentrations have the potential to be carcinogens (Bull and Kopfler 1991). Thus, a trade-off is needed to determine the minimum chlorine injection rate that achieves the required protection and minimize the potential health risks. The problem of determining the optimal chlorine dosing rate is called the "Chlorine Injection Problem". Based on previous work (Wable et al. 1991; Sharp et al. 1991), mass-transfer-based model was developed to predict the chlorine decay in water networks assuming first order reaction in both bulk flow of water and at the pipe wall. This model was then calibrated with measurements gathered from real network to update the reaction constant (Rossman et al. 1994).

An inverse method was developed by Islam et al. to determine the required time-varying chlorine injection at single source to maintain the disinfectant concentration fixed at selected node.

The differential equation describing chlorine transport was discretized using four-point implicit finite difference and solved simultaneously with the junction mass balance equations (Islam et al. 1997).

Boccelli et al. (1998) discussed the idea that using chlorine boosters at different locations within the network can reduce the total mass required compared to the conventional injection at the source. They introduced an optimization model formulated to determine the dynamic schedule of injection that minimizes the total dose required to maintain the residual chlorine concentration within the specified range. One scenario with injection at different three nodes allowed a reduction in disinfectant of 60.3% compared to the conventional injection at one source node (Boccelli et al. 1998).

Recently, especially after September 11, 2001 more concerns were directed towards identifying the source of a harmful contaminant that introduced intentionally or unintentionally to the water distribution systems. The problem is often known as the “Source Inversion Problem”.

An input-output model was first introduced by Zierolf et al. which described a constituent concentration at a given node and given time as a weighted average of exponentially decay values of the concentrations at all adjacent upstream nodes (Zierolf et al. 1998). Further improvement to this model was introduced by Shang et al. (2002) to allow adding storage tanks and multiple sources and quality inputs. This particle backtracking algorithm (PBA) was able to track a large number of water parcels simultaneously resulting in more efficient algorithm than proposed by Zierolf et al. (Shang et al. 2002). In 2005, Laird et al. introduced the origin tracking algorithm, an efficient water quality model appropriate for real-time applications.

To identify the contamination source(s), Laird et al. (2005) developed a nonlinear programming approach for the inverse problem. An unknown time-dependant injection term was introduced at every node and the inverse formulation solved for these profiles to identify the injection sources.

The solution was further refined by the same authors to search for unique solution by identifying the number of likely injection locations (Laird et al. 2006).

One major drawback of most of the research concerning water quality is that they assume known flow velocities in the links. In reality network demands are only loosely characterized using historical measurements and subjected to high uncertainty. The major focus of the research in this proposal is to provide accurate real-time estimates of the demands to support online monitoring, control, and other applications.



## **CHAPTER III**

### **HYDRAULIC MODELING IN WATER NETWORKS**

Modeling of water distribution systems can be classified into two main categories: hydraulic modeling and water quality modeling.

Hydraulic modeling refers to the mathematical description of pressure and flow within the system, whereas water quality modeling aims to determine the composition of the fluid within the system. Under the assumption that the changes of the composition of the fluid in the system are small enough that they do not affect the fluid flow properties, the hydraulic model and the quality model can be decoupled. The hydraulic model can be derived and solved independently, however it is still a necessary precursor to the water quality model. The work within this study focuses essentially on the hydraulic model.

Reliable distribution systems models are necessary for a number of purposes including the following:

- **New Design and Expansion:** Possible alternatives can be simulated to ensure adequate delivery capacity and appropriate system pressure. System designs can be optimized for cost, performance, and operation.
- **Operation of Existing Systems:** Given an existing system, the response to possible events can be simulated, removing the need to test these conditions in the real system, saving time and money. Furthermore, for situations where water quality is an issue, direct testing on the system may be difficult or hazardous.

Operation problems that require a reliable water quality model include optimal disinfectant control and contaminated detection and mitigation (Boccelli et al. 1998; Rossman et al. 1994; Guan et al. 2006; and Laird et al. 2006).

With most water quality models, it is necessary to first establish reliable estimation of the flow patterns in the network. This is usually difficult due to insufficient measurements data and a hydraulic modeling framework is required.

In the real life, water distribution networks are extremely complex and involve a large number of components (pipes, pumps, minor connections, consumption points, tanks, valves ....etc.). It is difficult to consider the exact geometry of all such components in the mathematical model. However, an acceptable level of accuracy can be achieved with a coarse network structure.

In this Chapter, the development of the hydraulic model is described for large water distribution systems. This starts with addressing the fundamental principles and assumptions followed by the basic mathematical models for different components in the network.

### **3.1 Modeling Fundamentals and Assumptions**

This section discusses the basic terminologies, hydraulic principles, and the assumptions used in hydraulic modeling of water distribution system. For more details on modeling fundamentals and basic principles for water networks, several good texts exist (Walski et al. 1990; Cesario 1995; and Bhave 2003).

Water distribution systems consist of pipes, pumps, and valves that convey water from source points such as reservoirs, tanks, and storage facilities to consumers at the consumption points.

The system can be represented as a network with nodes representing water sources, junctions, or consumption points. The links represent the pipes, pumps, and valves. A schematic diagram for a water network system is illustrated in Figure 3-1.



Under these assumptions, the hydraulic models for the network can be derived using the standard mass conservation law and the mechanical balance form of the energy conservation law. The latter is described through hydraulic grade lines

### 3.1.1 Mechanical Energy Balance

Consider the energy balance for the flow of water in a pipe as shown below in Equation 3-1.

$$\Delta U + \Delta E_k + \Delta E_p = Q + W \quad (3-1)$$

$\Delta U$ : Change in Internal Energy ( $= m \hat{\Delta U}$ )

$\Delta E_k$ : Change in Kinetic Energy ( $= \frac{m}{2g_c} \Delta v^2$ )

$\Delta E_p$ : Change in Potential Energy ( $= m \frac{g}{g_c} \Delta Z$ )

$Q$ : Energy Flow to The System

$W$ : Work Done on The System ( $= W_f + W_s$ )

$$W_f = m_{in} \hat{V}_{in} P_{in} - m_{out} \hat{V}_{out} P_{out}$$

The term “ $W_s$ ” refers to the work done by a moving part such as an external shaft, while “ $W_f$ ” refers to the work done by the fluid. For the flow of water in a pipe, the inlet and the outlet mass are the same based on the assumption that the consumption of water occurs only at the nodes. Due to incompressibility of water, the specific volume of the inlet and the outlet stream are the same. Thus, the last equation can be written as follows:

$$W_f = m \hat{V} (P_{in} - P_{out}) = -m \frac{\Delta P}{\rho} \quad (3-2)$$

With the assumption that the velocity change is negligible and using the expression mentioned above, Equation (3-1) can be rewritten as:

$$\frac{\Delta P}{\rho} + \frac{g}{g_c} \Delta Z + \left( \Delta \hat{U} - \frac{Q}{m} \right) = \frac{W_s}{m} \quad (3-3)$$

The two terms in brackets ( $\Delta U - Q/m$ ) are commonly referred to as the friction term  $E_F$ , and the last equation can be written as:

$$\frac{\Delta P}{\rho} + \frac{g}{g_c} \Delta Z + E_F = \frac{W_s}{m} \quad (3-4)$$

Equation (3-3) is known as the Mechanical Energy Balance equation. When describing the flow of water in a pipe, there is no shaft work and the last term in the right hand side vanishes. If the difference in pressure and the elevations are not enough to drive the water from point to another, a pump might be used. In this case, the last term in the right hand side expresses the power added by the pump.

### 3.1.2 Hydraulic Grade Lines

As discussed in the previous section, energy of water at any point in the distribution system can be expressed as one or combination of *Potential energy*, *Kinetic energy* and *Pressure energy*. *Potential energy* is associated with position or elevation above a pre-defined datum. *Flow energy*, usually named as *Pressure energy*, refers to the work that water can do on the surroundings. *Kinetic energy* is the energy due to the water velocity.

In water network applications, it is more common to express the energy in terms of head. Thus, the total water energy at a point in the system is the sum of the elevation head ( $Z$ ), the pressure head  $H_p$  and the velocity head  $v^2/2g$ .

A line of the total head plotted against distance along the system links (pipes) is called the energy grade line (EGL), while neglecting the velocity head produces the hydraulic grade line (HGL).

Thus, the hydraulic grade line is always below the energy grade line by the value of the velocity head. Because the velocity head can be neglected in most of the water applications, the analysis and the design of the water distribution system is commonly based on the hydraulic grade line instead of the energy grade line. (Walski et al. 2001)

It is also worth to mention that the energy grade line is only horizontal (i.e. constant energy line) in static systems or in flow systems in which the head due to the friction losses is considered negligible. The concept of the energy grade line and the hydraulic line is shown in Figure 3-2.

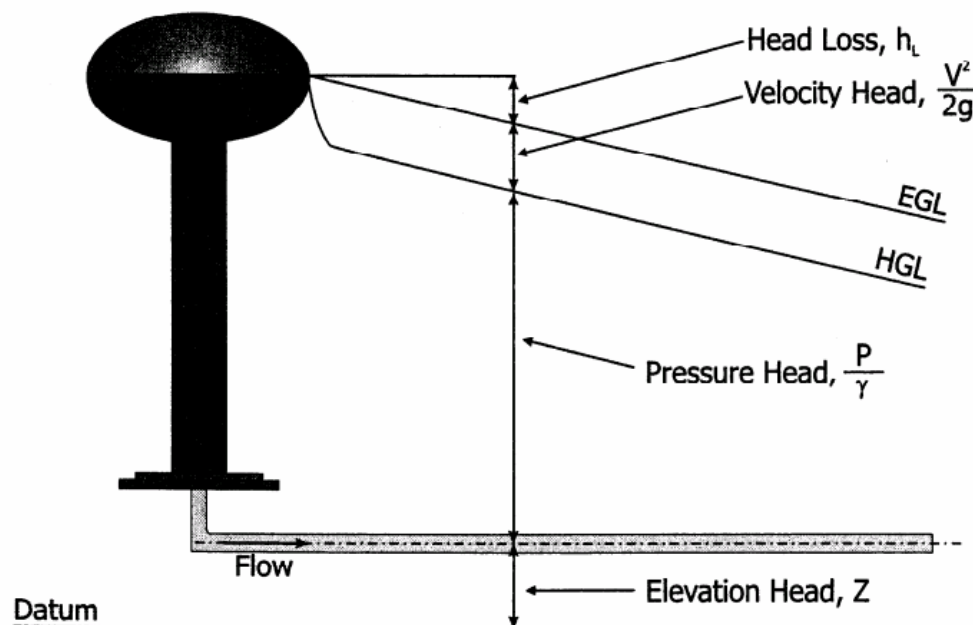


Figure 3-2: Schematic Diagram Showing the Energy Grade Line (EGL) and the Hydraulic Grade Line (HGL), (Walski et al. 2001).

It is more common and convenient in water network modeling to describe each term in units of head rather than units of energy.

$$H_{P1} + Z_1 + h_P = H_{P2} + Z_2 + h_L \quad (3-5)$$

$H_p$ : Pressure head

$Z$ : Elevation

$h_p$ : Pump head

$h_L$ : Friction losses head

Subscripts 1, 2 refer to the inlet and the outlet points in the pipes.

### 3.2 Distribution System Component Models

In water network modeling, several components should be considered. These components can be classified as physical components (e.g. junctions and pipes) and non-physical components (e.g. demand pattern). The next section gives brief description of each type along with their mathematical formulation.

#### 3.2.1 Nodes

Nodes represent sources of supply (Reservoirs), storage facilities (Tanks) and network junctions which may or may not be consumption points.

##### *Reservoirs*

The term reservoir in water modeling represents nodes with infinite capacity to supply or accept water from the network while their hydraulic head remains constant. The term can be used to model similar types of water sources such as lakes or rivers. The reservoir is modeled as an infinite source and the only required information to define a reservoir within a hydraulic model is the elevation of the water surface ( $Z$ ). In our model we always assume the reservoir is open to the atmosphere and its associated head is zero ( $H_p = 0$ ).

The reservoir in our model is described by a simple mass conservation equation, while the energy balance equation does not provide any useful information since the temperature of the reservoir is assumed constant and there are no constitutive equations

The mass conservation equation that describes the flow from the reservoir to the water network system can be written as:

$$FR_r(t) - \sum_{k \in P_r^{Out}} F_k(t) = 0, \quad \forall r \in \text{Reservoirs} \quad (3-6)$$

$FR_r$  : The Inlet Flow to The Network from a Reservoir

$t$  : Time

$P_r^{Out}$  : The Set of Pipes Out from a Reservoir

$F_k(t)$  : Flow along pipe k

### *Tanks*

Tanks are the storage facilities within the network and they also represent boundary points. Water volume stored in tanks can vary with time during a simulation. The storage tank sizing in the water distribution systems is controlled by regulations that require utilities to deliver minimum quantity to customers.

Pump schedules or level controls typically govern the level in the tank. Here, we treat the pump state operation as a known input to the model.

The primary input properties for tanks are: bottom elevation at which water level is zero, diameter, initial water levels, and initial water quality. The principal output described by the model is the hydraulic head over time.



Because most of the water applications in water networks involve tanks with constant area, the mass conservation equation is often derived as a function of the water level in the tank rather than the amount accumulated.

$$\frac{dH_T(t)}{dt} = \frac{1}{A_T} * \left( \sum_{k \in P_T^{In}} F_k(t) - \sum_{k \in P_T^{Out}} F_k(t) \right), \forall T \in \text{Tanks} \quad (3-7)$$

$H_T$  : Water Level in The Tank

$A_T$  : Area of The Tank

$P_T^{In}$  : The Set of Inlet Pipes to The Tank

$P_T^{Out}$  : The Set of Outlet Pipes from The Tank

### *Junctions*

Junctions are points in the network where links join together and where water enters or leaves the network. A change in pipe diameter, and pump connections can be represented by junctions as well. In typical simulations, the inputs for each junction are the elevation and the water demand profile. Demand patterns are discussed later in this chapter. The typical output is the time profile of the hydraulic head.

Junctions are considered as zero volume elements and the summation of the flow entering a node is equal to the summation of the flow coming out plus the demand required at this node at any time point (t):

$$\sum_{k \in P_j^{In}} F_k(t) = \sum_{k \in P_j^{Out}} F_k(t) + d_j(t), \forall j \in \text{Nodes} \quad (3-8)$$

$P_j^{In}$  : Set of pipes flowing into Node j

$P_j^{out}$  : Set of pipes flowing out of Node j

$d_j(t)$ : Rate of Water Consumption (Demand) at Node j

### 3.2.2 Links

In addition to the node components, two types of components represent the links; *Pipes* and *Pumps*. A brief description of each follows in the next section.

#### *Pipes*

Pipes are the links that convey water from one point in the network to another. There are wide range of pipe materials that have been used for water distribution systems including cast iron, ductile iron, steel, concrete, PVC and asbestos. Selection of pipe material is determined by factors such as the hydraulic performance, strength, corrosion-resistance, requirements of maintenance, availability and cost.

The basic input parameters for pipes in the model are: start and end nodes, diameter, length, status (open or closed) and roughness coefficient. The latter is a critical factor for determining the head loss between two nodes. Model outputs for pipes include: flow rate, velocity, and head losses in time.

Based on assumption (1) mentioned in section 3.1.2, flow into pipe is equal to flow out and one variable  $F$  can represent the flow value along any cross section of the pipe as well as at the inlet and the outlet. Starting from the energy balance equation for a flow system, the final form of the mathematical formulation that describes the energy conservation through the pipes is the mechanical balance equation excluding the pump term as shown in Equation (3-8). A constitutive equation is needed to express the friction losses as a function of the pipe flow.

$$H_{P1} + Z_1 = H_{P2} + Z_2 + h_L \quad (3-9)$$

Pipes are assumed to be full at all times and fluid is assumed to be incompressible. Flow direction should always be from the end at which higher hydraulic head exists to the end with lower head. When modeling, we assume a particular flow direction. If this direction is correct, the flow value will be positive. As described latter, the model has been smoothed to handle negative flow values when flow is opposite to the assumed direction.

### Head Losses

Head losses in the water distribution system can be classified into two types: friction losses due to the flow in the pipes and the head losses due to minor or small connections. In most practical applications, the effect of the head losses due to the minor connections can be neglected compared to the friction losses or to be taken as a small percentage (5 to 10%) of the total friction loss (Behave 2003).

In typical simulation frameworks, friction losses can be estimated by one of three basic and common formulas. These are: (1) The Darcy-Weisbach formula; (2) The Hazen-William formula; and (3) The Manning formula.

The Darcy-Weisbach formula is a more physically-based formula derived from the basic governing equation of Newton's second law. Hence with appropriate estimation of the fluid viscosity and density, the friction losses for any Newtonian fluid can be estimated. However, the application of Darcy-Weisbach formula in the water modeling is more difficult and complex as it results in a highly non-linear expression that leads to numerical difficulty (Walski et al. 2001).

The Hazen-William and the Manning formula, on the other hand are empirical-based equations. Most of the recent studies recommend the use of Hazen-William formula due to its simplicity and based on the fact that it shows very good agreement with the Darcy-Weisbach formula especially for the turbulent flow region. The Hazen-William is the predominant equation used in the United

States for determining the friction losses in water distribution systems and thus it was selected for expressing the friction losses in the current work (Walski et al. 1990). Table 3-1 gives some estimated values for the Hazen-William coefficients for different pipe materials.

Hazen-William formula

$$h_L = \text{Resistance Coefficient (A)} * (F)^n \quad (3-10)$$

$$A = 4.727 * C^{-1.852} * D^{-4.871} * L \quad (3-11)$$

$h_L$  : head of the friction losses, (ft)

F : Volumetric waterflow, (cfs)

D : Pipe Diameter, (ft)

L : Pipe Length, (ft)

n = 1.852

C : Hazen Williams Roughness Coefficient

Table 3-1: Hazen-William Roughness Coefficient for Different Pipe Materials,  
(Rossman 2000)

Material	C, Unitless
Cast Iron	130-140
Concrete	120-140
Galvanized Iron	120
Plastic	140-150
Steel	141-150

### *Pumps*

Pumps are the elements that add energy to the system by increasing the head. Since water only flows “downhill” from higher energy to lower energy, pumps are used to increase the head at desired location to overcome the piping head losses and physical elevation differences. Because pumping systems are more costly than simply providing flow by gravity, pumps are used only when gravity can not provide adequate pressure difference.

In water distribution system, “velocity” pumps are more frequently used, including centrifugal pumps and vertical-turbine pumps. Practically, centrifugal pumps are favored for the following advantages: wide selection of flow capacity, uniform flow at constant speed and head, low initial cost and relatively low noise level. (Cesario 1995).

With the centrifugal pump type, performance is a function of flow rate. This performance can be described by four factors; head, efficiency, power and the required net positive suction head (NPSH). The principal input parameters for the pump model are its start and end nodes and its pump curve which represents the relation between head and flow that the pump can produce.

The principal output parameters are flow and head gain. Flow through a pump is unidirectional and it is possible in modeling to set the flow through the pump to zero for a specific period of operation or when certain conditions exist in the network.

The mass conservation equation just implies the equality of the inlet and the outlet flow. Therefore, as in the case of a pipe, one variable “F” can represent both. The energy balance equation can be written as:

$$H_{P1} + Z_1 + h_P = H_{P2} + Z_2 \quad (3-12)$$

Another constitutive equation describing the pump head as a function of flow is needed which is known as the Pump Head-Discharge Relationship.

### The Pump Head-Discharge Relationship

The relationship between the pump head and the pump discharge is given by what is called the head characteristic curve. As shown in Figure 3-3, this relationship is not linear. The head plotted in Figure 3-3 expresses the difference between the outlet head and the inlet head (i.e. the head gain through the pump).

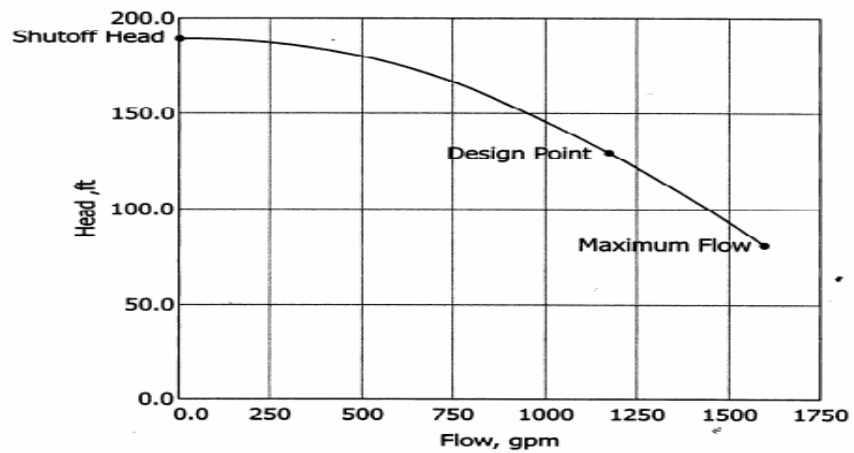


Figure 3-3: Pump Head-Discharge Curve, (Walski et al. 2001)

There are many ways to fit such relations in water modeling. Some models assume polynomial behavior, however the most common is the following power relation:

$$h_P = C_1 - C_2 * (F)^{C_3} \quad (3-13)$$

$h_P$  : Pump Head, (L)

$C_1$  : Cutoff (shutoff) head, (L)

$F$  : Water flow,  $(L/T^3)$

$C_2, C_3$  : Pump curve parameters.

A valid pump curve must have decreasing head with increasing flow. The water model in the current work can be adjusted to different shapes of pump curves depending on the number of points supplied.

Three (or more)-Point Curve: when three points (or more) on the pump curve are known, a continuous function of the form described in Equation (3-12) can be used to fit the data and estimate the three parameters in the pump equation  $C_1$ ,  $C_2$ ,  $C_3$ .

Single-Point Curve: in such case, only one point describing the relation between the head and the flow is defined. Based on technical practice, two more points are added:

- Maximum flow equal to twice the given flow is assumed at zero demand
- Shutoff head at zero flow equal to 133% of the given head.

Once  $C_1$ ,  $C_2$ , and  $C_3$  are defined for a particular pump,  $h_p$  is included in the model with these fixed parameters.

#### *Demand Pattern*

The flow rate of water out of the system to the consumers is a function of the system pressure and valve positions at every possible consumption point. However, this level of detail is very difficult to model and, since compressed node models are typically used, most simulations assume a known water demand profile at each node.

Usually the largest source of error in water modeling comes from the uncertainty in estimation of the water demands (Walski et al. 1990; Shang et al. 2006). Hence, the current work seeks to estimate these demands from online measurements.

According to the type of the analysis or the application required, data or estimates on the existing or future water consumption rates are required. One source of information is the billing records obtained from the different utilities. However this information is aggregated in time and is

not in the form that can be readily used in the model. Thus, determining the current water nodal demand or projection of these demands in future is required.

Nodal water demands are classified as domestic, public, commercial and industrial. Domestic use includes the usage in residential area for the routinely daily activities and is estimated as 30-50% of the total water consumption. Public use in places such as hospitals, restaurants, parks and schools, amounts to about 5-10% of the total water consumption. Commercial use includes water used in office buildings, restaurants, hotels and shopping centers and represents 10-30%. Industrial use is for manufacturing and processing purposes and accounts for 20-50% of the total water demands (Bhave 2003). The process of determining water demands includes the following (Walski et al. 2001):

- Estimation of the average-day demand.
- Determining the peak factor of the maximum rate.
- Estimation of the diurnal pattern for the extended period simulation (EPS).
- Projection of these demands in future.

The peak factor represents the ratio between the maximum-day and the average-day demand. It is estimated in the range of 1.2 to 3. For unsteady state applications (or the extended period simulation), the time profile describing the hourly demand pattern is required. Figure 3-4 shows a typical example of such profile for a residential area



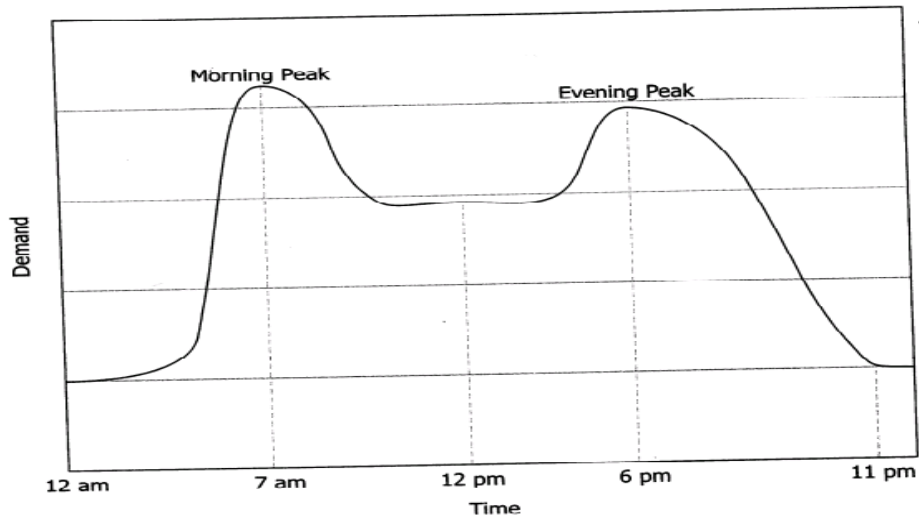


Figure 3-4: Schematic Diagram for the Nodal Demand Daily Distribution, (Walski et al. 2001)

In water modeling, this pattern can be introduced to the model as set of demands versus time at each node; however one shortcoming of this definition is that it does not offer much flexibility to reuse such data with a similar pattern but with different average demands. Therefore, a baseline of the average-day demand is defined separately for each node. Then, this base demand is multiplied by demand-pattern factor at each time interval. A typical interval used for the demand pattern is 1 hour which is referred to as the “hydraulic time step”.

## CHAPTER IV

### PROBLEM DEFINITION AND MATHEMATICAL FORMULATION

This chapter provides a detailed problem statement and discussion of the mathematical formulation and the solution methodology,

#### 4.1 Problem Definition

As mentioned in chapter I, the various solution methodologies for the many water quality applications assume known consumer water demands. Typically, the network flows and pressures are obtained by simulating the water distribution system using one of the water network simulation software packages such as EPANET, WATSIM, AQUA and WADISO, with the assumed demands treated as real inputs. In reality, these demands are loosely characterized. Estimation of water demands has always been a critical key factor in water network modeling.

Estimates of these demands are often obtained from historical billing records or estimated based on previous engineering experience with similar networks. In case of design a new networks, the engineering estimation is the only source for the water consumption rates (Walski et al. 1990). Unfortunately, spatially diverse measurements (e.g. billing records) are aggregated in time, while measurements that are frequent in time are only taken at a few points within the network. Further, even if sufficient information existed, there is significant uncertainty in specific real-time consumer demands.

Effective control, operation, and online optimization rely on reliable real-time estimates of the network flows. Accordingly, this work aims to provide a technique by which network flows and pressures can be estimated using the sparse flow and pressure measurements, coupled with historical demand estimates. To accomplish this task, we setup a nonlinear parameter estimation problem with a least square objective function based on limited measurement error. This problem is inherently ill-posed. Since there are insufficient measurements, there is non-uniqueness associated with the estimation problem. Therefore, the objective function is modifies to include

deviation from the offline demand estimates as a problem regularization. This formulation is tested with three specific case studies. In this chapter, the optimization formulation is developed and the equation based model is validated against the EPANET simulator software.

## 4.2 Problem Formulation

The estimation problem is formulated as follows. The objective function is written as:

$$\min \frac{1}{\rho_P} \sum_{i \in \text{Nodes}} \sum_{j \in \text{Times}} \alpha_i * (P_i(t_j) - SP_i(t_j))^2 + \frac{1}{\rho_F} \sum_{k \in \text{Links}} \sum_{j \in \text{Times}} \beta_k * (F_k(t_j) - SF_k(t_j))^2 + \frac{1}{\rho_d} \sum_{i \in \text{Nodes}} \sum_{j \in \text{Times}} \omega_i * (d_i(t_j) - Sd_i(t_j))^2 \quad (4-1)$$

where:

$\rho$       Weighting factors

$\alpha, \beta, \omega$    Binary parameters to identify the node or link with available measurements.

$SP_i$       The pressure measurement at node I, if available

$SF_k$       The flow measurement at link k, if available

$Sd_i$       The assumed demand at node i based on offline estimates.

The hydraulic model described in the previous chapter comprises the optimization constraints as follows:

### *Material Balance Conservation Laws*

These are the equations that describe the mass conservation around components such as reservoirs, junctions, and tanks.

Reservoirs:

$$FR_r(t) - \sum_{k \in P_r^{Out}} F_k(t) = 0, \quad \forall r \in \text{Reservoirs} \quad (4-2)$$

Junctions:

$$\sum_{k \in P_j^{In}} F_k(t) - \sum_{k \in P_j^{Out}} F_k(t) - d_j(t) = 0, \quad \forall j \in \text{Junctions} \quad (4-3)$$

Tanks:

$$\frac{dM_T(t)}{dt} = \rho \omega * \left( \sum_{k \in P_T^{In}} F_k^{in}(t) - \sum_{k \in P_T^{Out}} F_k^{out}(t) \right), \quad \forall T \in \text{Tanks} \quad (4-4)$$

$$\frac{dHT_T(t)}{dt} = \frac{1}{A_T} * \left( \sum_{k \in P_T^{In}} F_k^{in}(t) - \sum_{k \in P_T^{Out}} F_k^{out}(t) \right), \quad \forall T \in \text{Tanks} \quad (4-5)$$

*Mechanical Energy Balance conservation laws*

$$H_p^{in}(t) + Z(t) \frac{in}{p} + hP_p(t) = H_p^{out}(t) + Z \frac{out}{p}(t) + hL_p(t), \quad \forall p \in \text{Pipes} \quad (4-6)$$

In the above equation, the pump term  $hP$  in the left hand side and the friction losses term  $hL$  in the right hand side are described in Equations (3-1), (3-2) and (3-3).

As shown in Equation (4-1), the model formulates the objective function as a standard least squares error expression that minimizes the difference between the calculated values of the flows and the pressures and the measured values. With limited measurement information, the pure estimation problem is ill-posed and requires regularization to ensure a unique solution. Therefore, the third term in the objective function regularizes the problem using offline demand estimates.

The weight of the first two terms that represent the measurement information is much higher than the regularization term.

Equations (4-2) to (4-5) describe the material balance equations for the different components in the network; junctions, reservoirs and tanks, while Equation (4-6) is a general form describing the energy conservation law in the links.

### 4.3 Challenges

The mathematical formulation shown earlier in section 4.2, presents challenges when these equations are applied to a real-world water network. This section addresses these situations and the formulations to consider each one of them

#### 4.3.1 Discretization for the ODE in Tanks

As shown in Equation (4-4) and (4-5), the material balance around the tank is described by a linear differential equation. Given the slow dynamics in the tank, an explicit Euler method was used to discretize the original equation in the time domain as follows:

$$HT_T(t_{j+1}) = HT_T(t_j) + (t_{j+1} - t_j) * \frac{1}{A_T} * \left( \sum_{k \in P_T^{In}} F_k(t_j) - \sum_{k \in P_T^{Out}} F_k(t_j) \right) \quad (4-7)$$

These discretized differential equations are included in the optimization formulation as constraints. The remaining algebraic equations are also discretized and added as constraints for each point in time.

### 4.3.2 Unknown Flow Direction

As mentioned in Chapter III, Hazen-William equation is the predominate equation used to express the head losses due to friction in North America. Reviewing Equation (3-3), it is clear that this formula does not accept negative values for the flows being calculated. However, negative values are commonly used when the flow direction at the solution is opposite to the assumed direction. In our optimization model, the magnitude and the direction of the flows are to be calculated. Therefore, the head loss equation was modified as follows:

$$|hL| = \text{Resistance Coefficient (A)} * (|\text{Flow}|)^n \quad (4-8)$$

The above equation aims to calculate the magnitude of the head losses as a function of the absolute values of the calculated flow. Then a conditional if-statement was added to the model in such a way to accept the positive of this expression if the calculated flow is in the right direction (i.e +ve value) or flip the sign to negative if the calculated flow is in the opposite direction to the assumed direction (i.e -ve value). Although this model contains a discrete switch, the transition across zero is smooth. The resulting relationship for the head loss is shown in Figure 4-1.

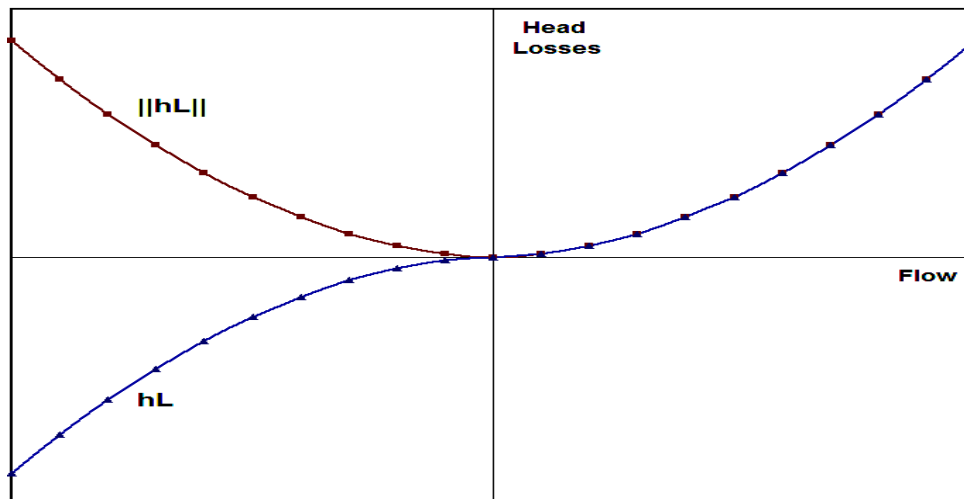


Figure 4-1: Adjusting the Flow Direction in the Model

### 4.3.3 Pump Switching and Tank Level Control

It is common to operate network pumps in different types of operational scheduling. Some of these patterns include:

- Pump operates on a pre-specified daily schedule.
- Pump operation is controlled by the tank level.
- Pump closes when the level reaches certain maximum height,  $H_{\max}$

Regardless of the control strategy, and because the problem is formulated as an estimation problem, the status of the pump at each point in time is known. Therefore, a binary input parameter (CSP) is included to indicate the status of the pump. A value of 1 is to be assigned to this parameter if the pump is open and a value of 0 if it is closed. The following expressions are used to account for pump switching.

$$Set \ CSP [ m , j ] = \begin{cases} 1, & \text{The Pump is open} \\ & P_m^{in} + Z_m^{in} + hP_m^{in} = P_m^{out} + Z_m^{out} , \forall m \in Pumps \\ 0, & \text{The Pump is closed} \\ & F [ m , j ] = 0 \end{cases}$$

#### 4.4 Validation of the Optimization Model

Before attempting estimation of the flows and pressures using the aforementioned formulation, the model is validated against existing simulation software EPANET (Rossman 2000). This model validation step tests the ability of the optimization formulation to solve for the true flows and pressures given the actual demand data.

Because it is currently difficult to obtain the real demand data from a real-world network, EPANET is used to represent the real distribution system. Based on the constraints described in Equations (4-2) to Equation (4-8), the degrees of freedom of the problem can be determined as the number of the junctions in the network. This idea is illustrated more in Table 4-1.

Table 4-1: Degrees of Freedom Analysis for Hydraulic Calculations in Water Networks

Network Component	Associated No. of Variables	Associated No. of Equation
( r ) Reservoir	r- flows from reservoir	r- Material Balance Equations
( j ) Junctions	j- demands & j- pressure heads	j- Material Balance Equations
( T ) Tanks	T- tank heads	T- Material Balance Equations
( P ) Links	P- flows in each link	P- Mechanical Balance Equations
Total	$( r + 2j + T + P )$	$( r + j + T + P )$
No. of D.O.F = $( r + 2j + T + P ) - ( r + j + T + P ) = j =$ No. of junctions		



To perform the validation step, simulations are run using EPANET with a specified demand pattern. The same demand pattern is specified in the model in the third term of the objective function. The weights for the remaining terms are set to zero. The numerical results from EPANET and the optimization formulation model are compared. This process is illustrated in Figure 4-2.

Chapter V provides a complete discussion of the model validation results, which show very good matching between the optimization formulation and EPANET.

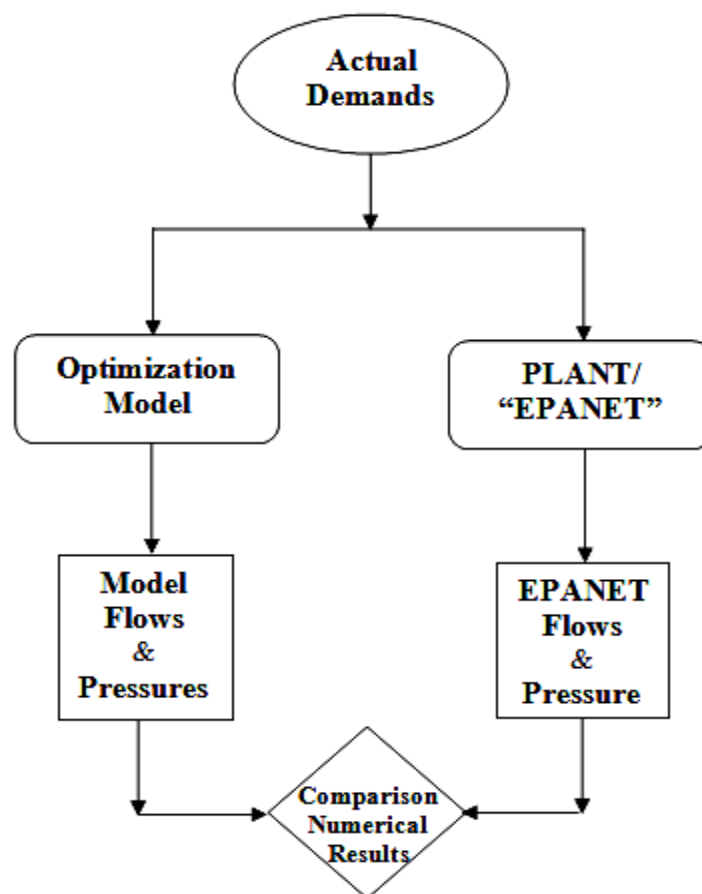


Figure 4-2: A Schematic Diagram for the Validation Problem

## CHAPTER V

### MODEL VALIDATION

In this chapter, the optimization model described in section 4-2 is validated against the results obtained from the water network simulation software “EPANET”. The development of the rest of the chapter proceeds as follows; first, the basic concept of the validation step is explained and described in a mathematical formulation. Second, three networks of different sizes and hydraulic features are chosen as cases studies and simulations are developed using EPANET. Finally, the optimization formulation is solved in a simulation mode and the results are compared with EPANET.

#### 5.1 Validation Formulation

This section describes the formulation used to validate the optimization model against EPANET. As mentioned earlier, the degrees of freedom in the water network model is the same as the number of the nodes excluding the reservoirs and the tanks (i.e. the number of junctions). In EPANET, these degrees of freedom are specified by specifying demand profile (pattern) at each node. In the model, these demands are “specified” through a least squares term in the objective function.

Accordingly, the mathematical formulation shown earlier in Equation (4-1) describing the full mode of optimization is modified as follows:

$$\min_{Pd} \frac{1}{\rho d} \sum_{i \in Nodes} \sum_{j \in Times} \omega_i * (d_i(t_j) - Sd_i(t_j))^2 \quad (5-1)$$

Demand profile is specified through the parameter  $Sd_i(t_j)$ . The optimal objective value of this problem should be zero, that is when  $d_i(t_j) = Sd_i(t_j)$ . In this fashion, the optimization formulation is tested in a simulation mode and the solution of the remaining variables can be compared with the simulation results from EPANET.

## 5.2 Case Studies

Three case studies were developed using the 3 network examples that come with EPANET package. These three networks represent different sizes and hydraulic features over a range of operational conditions. In the following sections, the features of each of these examples are described in detail

### 5.2.1 Case Study 1

A schematic diagram of the first network is illustrated in Figure 5-1. As shown in the figure, the network consists of 11 nodes; 9 junctions, 1 reservoir and 1 tank. The nodes are interconnected through 13 links; 12 pipes and 1 pump. Node (9) represents the water source (i.e. the reservoir) which feeds the rest of the network through pump (9). Water level in Tank (2) is controlled by manipulating the water flow from pump (9). Tables 5-1 and 5-2 show the specifications of the physical infrastructure as well as the different simulation parameters. The changes in demand at any node can be described by the “demand multiplier”. It is assumed that all demands in Case Study 1 follow the same demand pattern as shown in Figure 5-2.

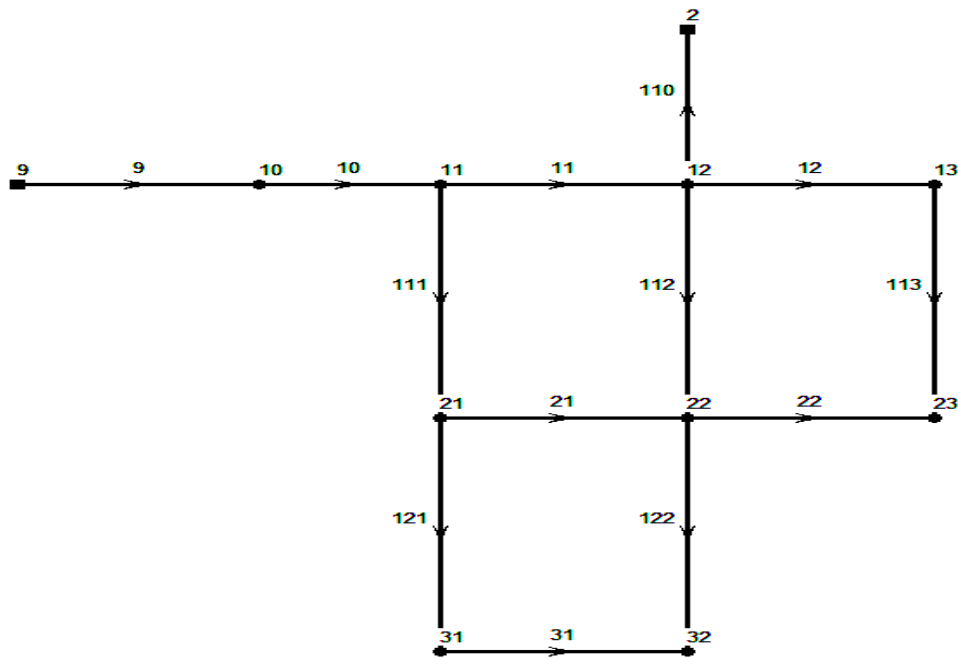


Figure 5-1: A Schematic Diagram for Case Study 1

Table 5-1: Input Data for Nodes in Case Study 1

Node	Type	Elevation, [ft]	Base Demand, [gpm]
2	Tank	850	N/A
9	Reservoir	800	N/A
10	Junction	710	0
11	Junction	710	150
12	Junction	700	150
13	Junction	695	100
21	Junction	700	150
22	Junction	695	200
23	Junction	690	150
31	Junction	700	100
32	Junction	710	100

Table 5-2: Input Data for Links in Case Study 1

Link	Type	Inlet Node	Outlet Node	Length, [ft]	Diameter, [in]	Roughness Coefficient
9	Pump	9	10	N/A	N/A	N/A
10	Pipe	10	11	10530	18	100
11	Pipe	11	12	5280	14	100
12	Pipe	12	13	5280	10	100
21	Pipe	21	22	5280	10	100
22	Pipe	22	23	5280	12	100
31	Pipe	31	32	5280	6	100
110	Pipe	2	12	200	18	100
111	Pipe	11	21	5280	10	100
112	Pipe	12	22	5280	12	100
113	Pipe	13	23	5280	8	100
121	Pipe	21	31	5280	8	100
122	Pipe	22	32	5280	6	100

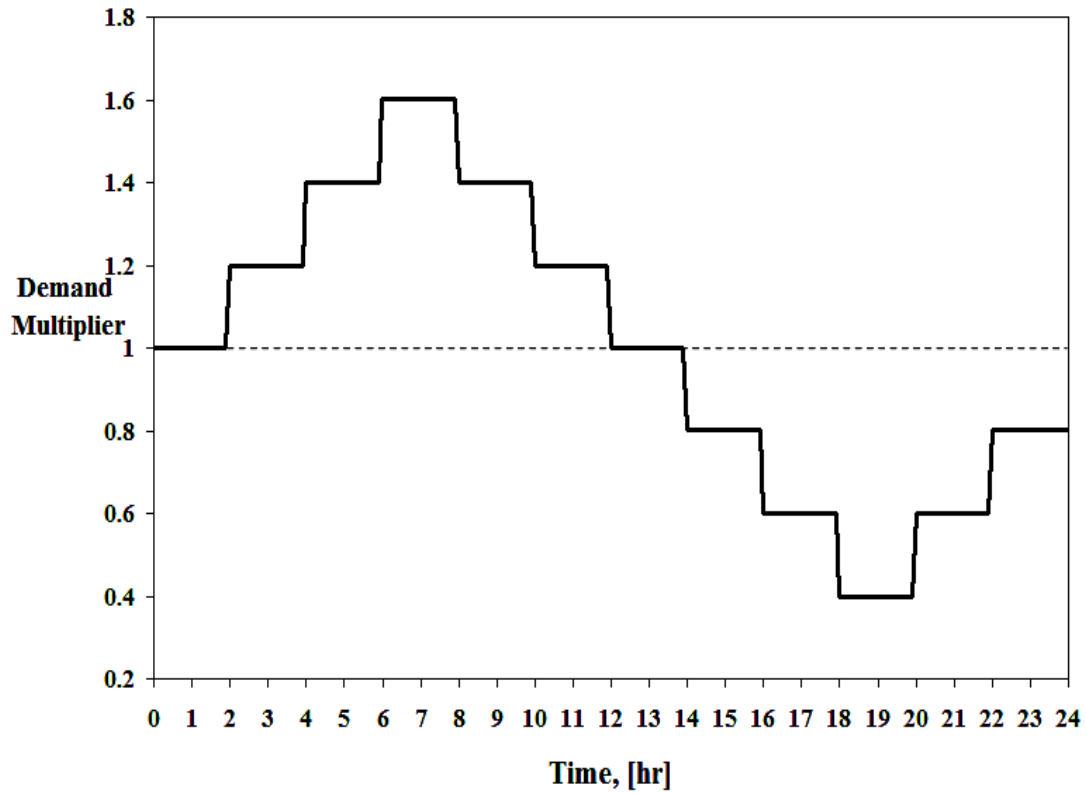


Figure 5-2: Demand Pattern in Case Study 1

### 5.2.2 Case Study 2

This case study is a network with 36 Nodes; 35 Junctions and 1 Tank. Although there is no reservoir (Lake or River), water is fed into the network through a pump station which is lumped into one inlet Junction; Junction (1). Water flows through 40 links. No pumps or other valves are included. Figure 5-3 describes the topography of the water network, while Tables 5-3 and 5-4 show representative input data for some selected nodes and links.

Table 5-3: Input Data for Selected Nodes in Case Study 2

Node	Type	Elevation [ft]	Base Demand [gpm]
1	Junction	50	0
2	Junction	100	8
3	Junction	60	14
11	Junction	185	34.78
12	Junction	210	16
13	Junction	210	2
16	Junction	150	20
17	Junction	180	20
23	Junction	230	8
24	Junction	190	11
35	Junction	110	0
36	Junction	110	1
26	Tank	235	N/A

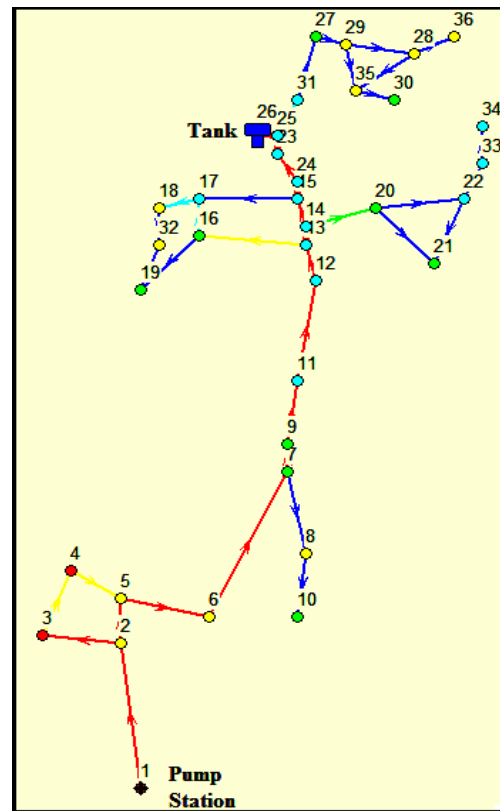


Figure 5-3: Layout of Case Study 2

Table 5-4: Input Data for Selected Links in Case Study 2

Link	Type	Inlet Node	Outlet Node	Length, [ft]	Diameter, [in]	Roughness Coefficient
1	Pipe	1	2	2400	12	N/A
2	Pipe	2	5	800	12	100
3	Pipe	2	3	1300	8	100
11	Pipe	9	11	700	12	100
12	Pipe	11	12	1900	12	100
13	Pipe	12	13	600	12	100
17	Pipe	15	17	1500	8	100
18	Pipe	16	17	600	8	100
26	Pipe	24	23	600	12	100
27	Pipe	15	24	250	12	100
29	Pipe	25	26	200	12	100
40	Pipe	28	35	700	8	100

### 5.2.3 Case Study 3

Taken from a real-world system, case study 3 has a dual-source configuration (Lake & River). This network consists of 96 Nodes including 91 Junctions, 2 Reservoirs, and 3 Tanks. Water flows in 117 Links of which 115 are Pipes and 2 are Pumps. Figure 5-4 is a schematic diagram for the network.

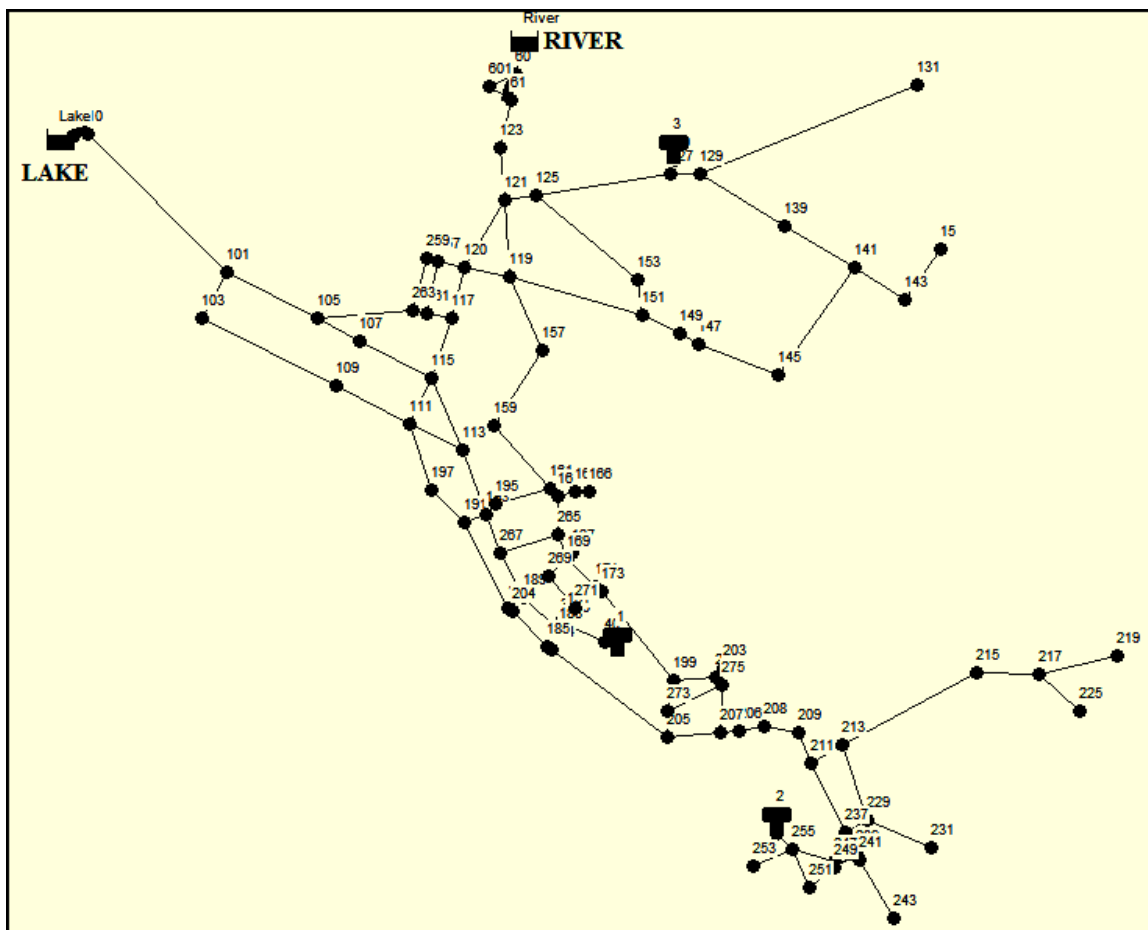


Figure 5-4: A Schematic Diagram for Case Study 3

The lake source is used only at specific times in the 24-hr period based on the status of pump (1). Water level in Tank (1) is controlled by Pump (335). Tables 5-5 and 5-6 give representative information about the network.

Table 5-5: Input Data for Selected Nodes in Case Study 3

Node	Type	Elevation [ft]	Base Demand [gpm]
River	Reservoir	220	N/A
Lake	Reservoir	167	N/A
1	Tank	132	N/A
2	Tank	116.5	N/A
3	Tank	129	N/A
10	Junction	147	0
15	Junction	32	1
20	Junction	129	0
101	Junction	42	190
103	Junction	43	133.2
151	Junction	33.5	144.48
153	Junction	66.2	44.17
213	Junction	7	13.94
215	Junction	7	92.19
217	Junction	6	24.22
271	Junction	6	0
273	Junction	8	0
275	Junction	10	0



Table 5-6: Input Data for Selected Links in Case Study 3

Link	Type	Inlet Node	Outlet Node	Length, [ft]	Diameter, [in]	Roughness Coefficient
10	Pump	Lake	10	N/A	N/A	N/A
35	Pump	60	60	N/A	N/A	N/A
20	Pipe	3	20	99	99	199
40	Pipe	1	40	99	99	199
50	Pipe	2	50	99	99	199
60	Pipe	River	60	1231	24	160
151	Pipe	15	143	1650	8	130
247	Pipe	213	215	4285	16	130
249	Pipe	215	217	1660	16	130
321	Pipe	163	265	1200	30	140
323	Pipe	201	275	300	12	130
325	Pipe	269	271	1290	8	130
329	Pipe	61	123	45500	30	140

### 5.3 Validation Results

In this section, numerical as well as graphical comparisons are used to demonstrate the level of agreement between the optimization model and EPANET.

#### 5.3.1 Validation Results for Case Study 1

Tables 5-7, 5-8 and 5-9 show the numerical results for the flow rates of selected Links (10, 112, 31). In Table 5-7 we can see the effect of the pump status and the high level of agreement between the optimization formulation and EPANET. Similar agreement is shown in Tables 5-8 and 5-9.

Table 5-7: Water Flow Rates in Link (10) in Case Study 1

Time [hr]	EPANET Flow [GPM]	Model Flow [GPM]	error	%error
0	1866.18	1866.156	1.26E-05	0.001265
1	1848.58	1848.564	8.55E-06	0.000855
2	1837.46	1837.445	8.05E-06	0.000805
3	1825.38	1825.369	5.97E-06	0.000597
4	1819.86	1819.842	1.02E-05	0.001017
5	1813.25	1813.239	6.12E-06	0.000612
6	1813.13	1813.116	7.89E-06	0.000789
7	1811.87	1811.856	7.95E-06	0.000795
8	1804.29	1804.278	6.93E-06	0.000693
9	1798	1797.989	5.95E-06	0.000595
10	1785.48	1785.471	5.15E-06	0.000515
11	1774.3	1774.298	1.18E-06	0.000118
12	1757.04	1757.033	4.15E-06	0.000415
13	0	0	0	0
14	0	0	0	0
15	0	0	0	0
16	0	0	0	0
17	0	0	0	0
18	0	0	0	0
19	0	0	0	0
20	0	0	0	0
21	0	0	0	0
22	0	0	0	0
23	1909.42	1904.66	0.002493	0.249311
24	1892.24	1887.536	0.002486	0.248578

An easier way to visualize the agreement is through a comparison plot. Figures 5-5 and 5-6 show the normalized flow rate values from the EPANET simulator on the x-axis, and the normalized values from the optimization formulation on the y-axis for the rest of the flows in the network. All points that lie on or close to the 45-degree line indicate excellent agreement. Figures 5-7, 5-8 and 5-9 show this comparison for pressures and tank level.

Table 5-8: Normalized Flow in Link (112) in Case Study 1

<b>Time [hr]</b>	<b>EPANET Flow [GPM]</b>	<b>AMPL Flow [GPM]</b>	<b>  error  </b>	<b>%error</b>
0	188.7	188.6996	2.12E-06	0.000212
1	191.73	191.7375	3.91E-05	0.003912
2	293.98	293.9813	4.42E-06	0.000442
3	295.94	295.9462	2.1E-05	0.002095
4	394.39	394.3882	4.56E-06	0.000456
5	395.4	395.4061	1.54E-05	0.001543
6	490.85	490.8529	5.91E-06	0.000591
7	491.04	491.0372	5.7E-06	0.00057
8	396.78	396.7855	1.39E-05	0.001386
9	397.75	397.7519	4.78E-06	0.000478
10	302.41	302.409	3.31E-06	0.000331
11	304.21	304.2107	2.3E-06	0.00023
12	207.4	207.4013	6.27E-06	0.000627
13	403.07	403.0684	0	0
14	322.45	322.4547	0	0
15	322.45	322.4547	0	0
16	241.84	241.841	0	0
17	241.84	241.841	0	0
18	161.23	161.2273	0	0
19	161.23	161.2273	0	0
20	241.84	241.841	0	0
21	241.84	241.841	0	0
22	322.45	322.4547	0	0
23	75.66	76.5613	0.011913	1.19125
24	184.18	184.9957	0.004429	0.442882

Table 5-9: Normalized Flow in Link (31) in Case Study 1

<b>Time [hr]</b>	<b>EPANET Flow [GPM]</b>	<b>AMPL Flow [GPM]</b>	<b>  error  </b>	<b>%error</b>
0	40.81	40.8101	2.45E-06	0.000245
1	40.46	40.4642	0.000104	0.010381
2	42.22	42.2167	7.82E-05	0.007816
3	42.05	42.0522	5.23E-05	0.005232
4	45.52	45.5245	9.89E-05	0.009886
5	45.46	45.4636	7.92E-05	0.007919
6	49.99	49.9892	1.6E-05	0.0016
7	49.98	49.9816	3.2E-05	0.003201
8	45.38	45.3818	3.97E-05	0.003967
9	45.33	45.3251	0.000108	0.01081
10	41.53	41.5249	0.000123	0.01228
11	41.38	41.3817	4.11E-05	0.004108
12	38.75	38.7526	6.71E-05	0.00671
13	28.67	28.6677	0	0
14	22.93	22.9342	0	0
15	22.93	22.9342	0	0
16	17.2	17.2006	0	0
17	17.2	17.2006	0	0
18	11.47	11.4671	0	0
19	11.47	11.4671	0	0
20	17.2	17.2006	0	0
21	17.2	17.2006	0	0
22	22.93	22.9342	0	0
23	42.74	42.6035	0.003194	0.319373
24	41.33	41.2379	0.002228	0.222841

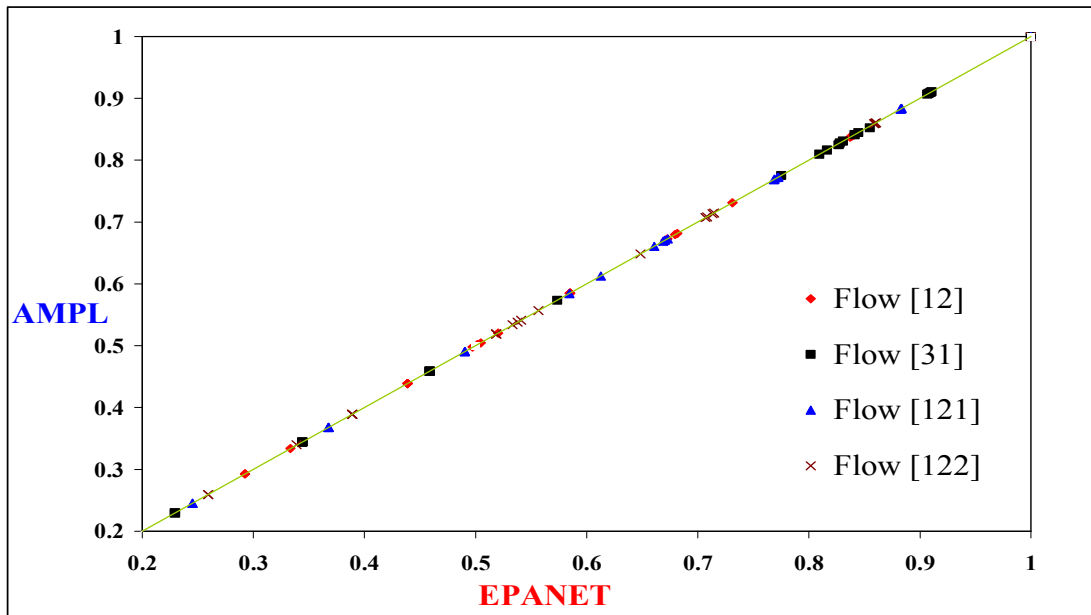


Figure 5-5: Normalized Flow in Links (12, 31, 121, and 122) in Case Study 1

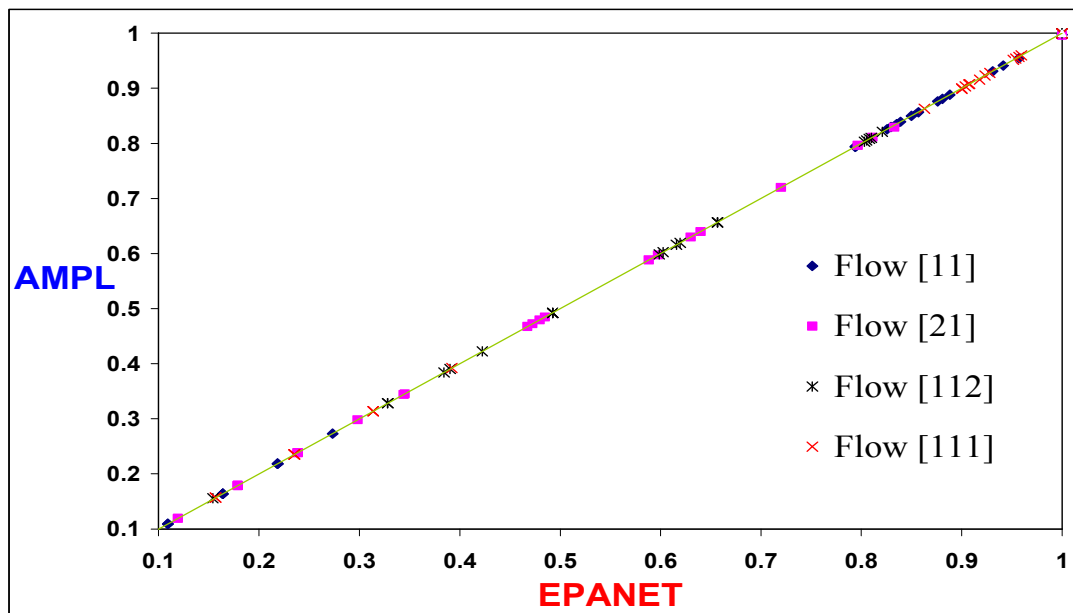


Figure 5-6: Normalized Flow in Links (11, 21, 111, and 112) in Case Study 1

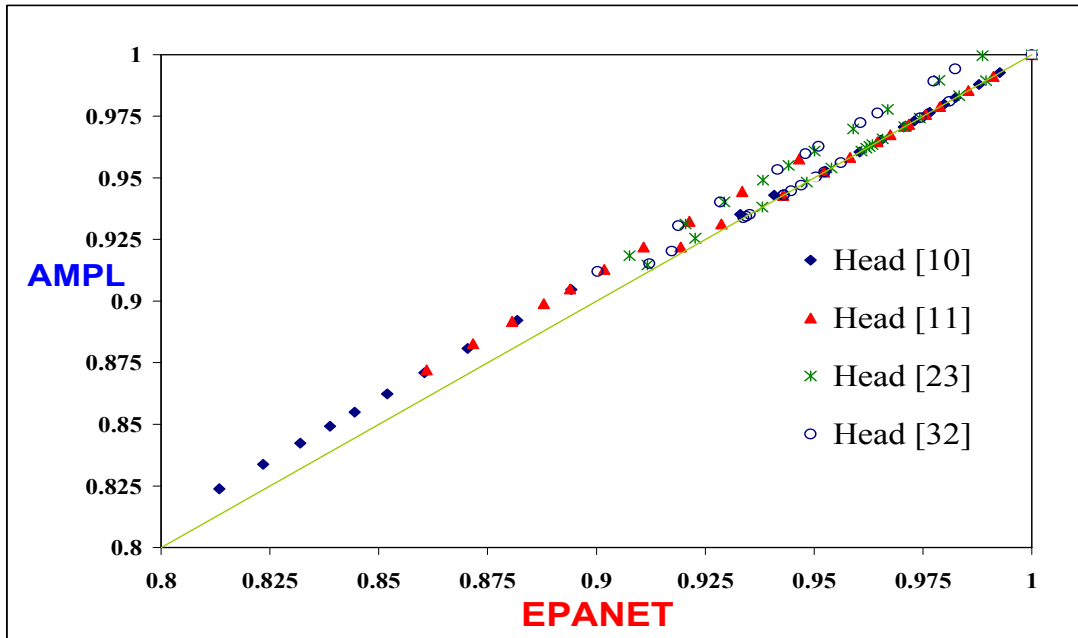


Figure 5-7: Normalized Head at Nodes (10, 11, 23, and 32) in Case Study 1

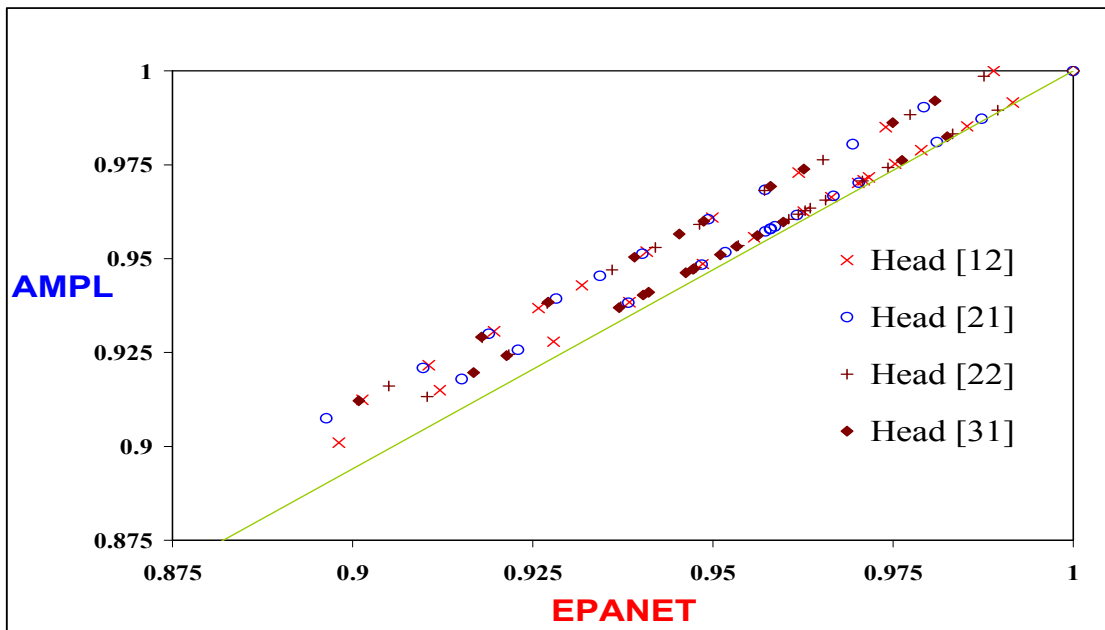


Figure 5-8: Normalized Head at Nodes (12, 21, 22, and 31) in Case Study 1

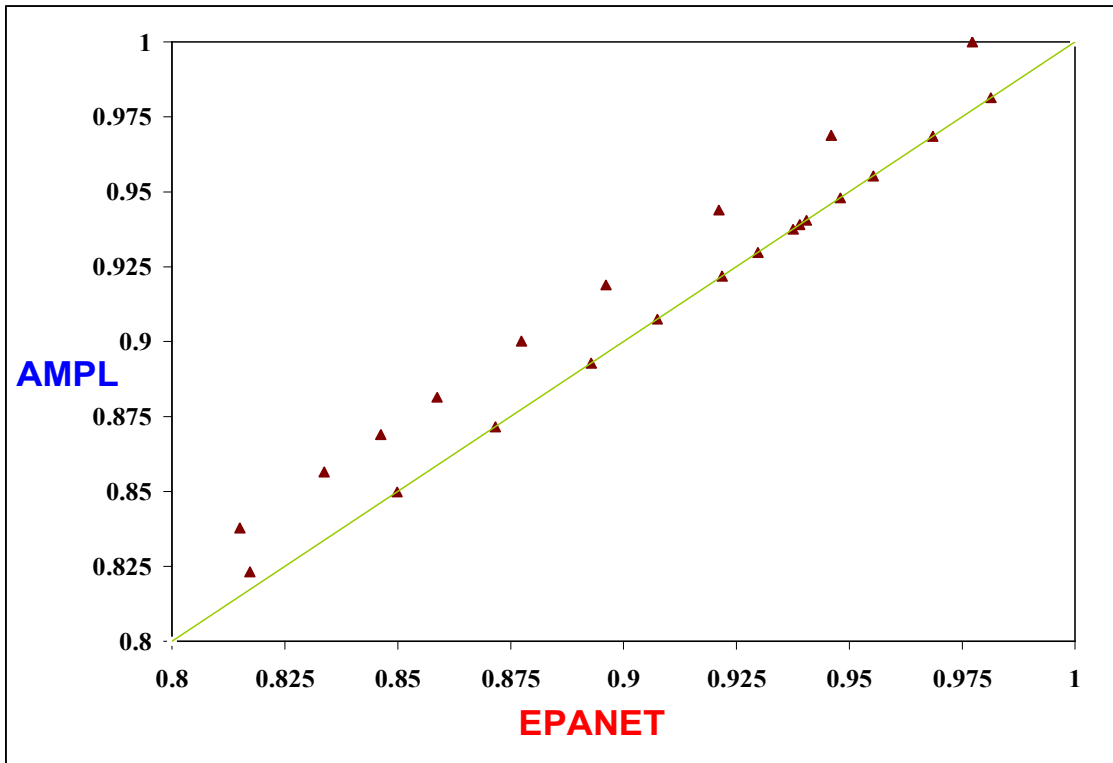


Figure 5-9: Normalized Level in Tank (2) in Case Study 1

### 5.3.2 Validation Results for Case Study 2

36 Nodes and 40 Links compose the structure of Network2. Tables 5-10, 5-11, and 5-12 compare the numerical results for pressure and flow at Node (20) and in Links (11) and (17) respectively.

Table 5-10: Normalized Head at Node (20) in Case Study 2

Time [hr]	EPANET	AMPL	Error	% Error
0:00	0.940143	0.940144	1.5348E-06	0.000163
1:00	0.950579	0.950576	3.0696E-06	0.000323
2:00	0.961783	0.961742	4.14396E-05	0.004309
3:00	0.972834	0.972823	1.07436E-05	0.001104
4:00	0.984882	0.984852	2.99286E-05	0.003039
5:00	0.9934	0.993413	1.30458E-05	0.001313
6:00	0.995779	0.995772	7.67401E-06	0.000771
7:00	0.993707	0.993664	4.29744E-05	0.004325
8:00	0.986877	0.986886	8.44141E-06	0.000855
9:00	0.974292	0.974272	1.99524E-05	0.002048
10:00	0.943903	0.943925	2.22546E-05	0.002358
11:00	0.939452	0.939461	8.44141E-06	0.000899
12:00	0.939682	0.939652	2.99286E-05	0.003185
13:00	0.956565	0.956537	2.83938E-05	0.002968
14:00	0.962628	0.962638	9.97621E-06	0.001036
15:00	0.979741	0.979728	1.22784E-05	0.001253
16:00	1	0.999995	4.6044E-06	0.00046
17:00	0.997698	0.997677	2.07198E-05	0.002077
18:00	0.993247	0.993223	2.37894E-05	0.002395
19:00	0.988029	0.987989	3.99048E-05	0.004039
20:00	0.976211	0.976244	3.37656E-05	0.003459
21:00	0.960018	0.960003	1.5348E-05	0.001599
22:00	0.948431	0.948437	6.13921E-06	0.000647
23:00	0.935692	0.935673	1.84176E-05	0.001968
24:00:00	0.933159	0.933128	3.14634E-05	0.003372
25:00:00	0.942829	0.942816	1.22784E-05	0.001302
26:00:00	0.952421	0.952427	6.13921E-06	0.000645
27:00:00	0.965467	0.96548	1.30458E-05	0.001351
28:00:00	0.976287	0.976317	2.99286E-05	0.003066
29:00:00	0.984959	0.984964	4.6044E-06	0.000467
30:00:00	0.994551	0.994538	1.30458E-05	0.001312
31:00:00	0.994705	0.994693	1.22784E-05	0.001234
32:00:00	0.983347	0.983327	2.07198E-05	0.002107
33:00:00	0.969688	0.969714	2.60916E-05	0.002691



Table 5-11: Normalized Flow in Link (11)

Time, [hr]	EPANET	AMPL	Error	% Error
0:00	0.852447	0.852453	5.95E-06	0.000596
1:00	0.877032	0.877038	5.95992E-06	0.000596
2:00	0.884854	0.88486	5.95992E-06	0.000596
3:00	0.884854	0.88486	5.95992E-06	0.000596
4:00	0.893794	0.8938	5.95992E-06	0.000596
5:00	0.86027	0.860276	5.95992E-06	0.000596
6:00	0.498443	0.49844	2.97996E-06	0.000298
7:00	0.074871	0.074871	0	0
8:00	0.074871	0.074871	0	0
9:00	0.149743	0.149743	0	0
10:00	0.274901	0.274901	0	0
11:00	0.108396	0.108396	0	0
12:00	0.724905	0.724905	0	0
13:00	0.958653	0.958653	0	0
14:00	0.874842	0.874842	0	0
15:00	0.966475	0.966475	0	0
16:00	1	1	0	0
17:00	0.068032	0.068032	0	0
18:00	0.041347	0.041347	0	0
19:00	0.074871	0.074871	0	0
20:00	0.140803	0.140803	0	0
21:00	0.174328	0.174328	0	0
22:00	0.132981	0.132981	0	0
23:00	0.140803	0.140803	0	0
24:00	0.502004	0.502004	0	0
25:00	0.82895	0.828947	2.97996E-06	0.000298
26:00	0.836773	0.83677	2.97996E-06	0.000298
27:00	0.870297	0.870294	2.97996E-06	0.000298
28:00	0.853535	0.853532	2.97996E-06	0.000298

Table 5-12: Normalized Flow in Link (17)

Time [hr]	EPANET	AMPL	Error	% Error
0:00	0.124406	0.124388	1.7917E-05	0.001792
1:00	0.042689	0.042652	3.73919E-05	0.003739
2:00	0.09496	0.094919	4.05079E-05	0.004051
3:00	0.094882	0.094919	3.73919E-05	0.003739
4:00	0.151593	0.151599	5.45299E-06	0.000545
5:00	0.074316	0.074279	3.73919E-05	0.003739
6:00	0.345174	0.345141	3.34969E-05	0.00335
7:00	0.272338	0.272351	1.3243E-05	0.001324
8:00	0.272338	0.272351	1.3243E-05	0.001324
9:00	0.544676	0.544702	2.64859E-05	0.002649
10:00	1	0.999975	2.49279E-05	0.002493
11:00	0.394329	0.394299	2.96019E-05	0.00296
12:00	0.006777	0.006813	3.58339E-05	0.003583
13:00	0.319389	0.319405	1.558E-05	0.001558
14:00	0.208148	0.208125	2.33699E-05	0.002337
15:00	0.36239	0.362395	5.45299E-06	0.000545
16:00	0.536652	0.536648	3.89499E-06	0.000389
17:00	0.25964	0.259605	3.50549E-05	0.003505
18:00	0.150425	0.150403	2.18119E-05	0.002181
19:00	0.272338	0.272351	1.3243E-05	0.001324
20:00	0.512191	0.512182	9.34798E-06	0.000935
21:00	0.634105	0.63413	2.57069E-05	0.002571
22:00	0.483758	0.483728	3.03809E-05	0.003038
23:00	0.512191	0.512182	9.34798E-06	0.000935
24:00	0.021189	0.021222	3.34969E-05	0.00335
25:00	0.04082	0.040813	6.23199E-06	0.000623
26:00	0.014801	0.014806	4.67399E-06	0.000467
27:00	0.227545	0.227552	6.23199E-06	0.000623
28:00	0.126431	0.126399	3.27179E-05	0.003272

Figures 5-10 and 5-11 combine the results for the other flows in the network, while Figures 5-12 and 5-13 show the comparison between the pressure head at the different Nodes. In addition, the water level in Tank (26) is illustrated in Figure 5-14.

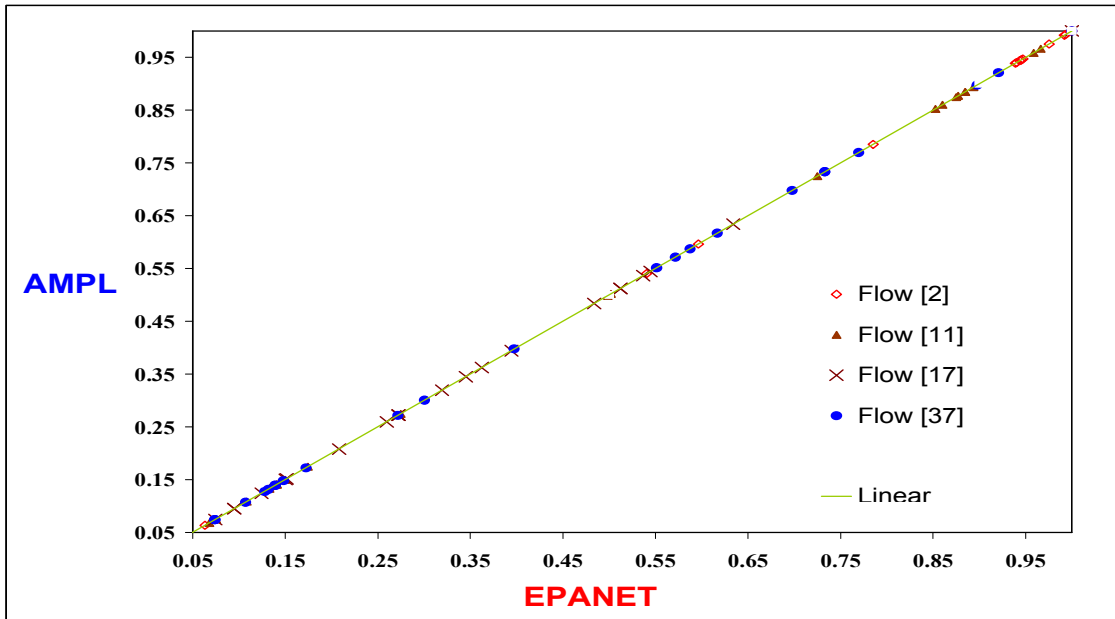


Figure 5-10: Normalized Flow in Links (2, 11, 17, and 37) in Case Study 2

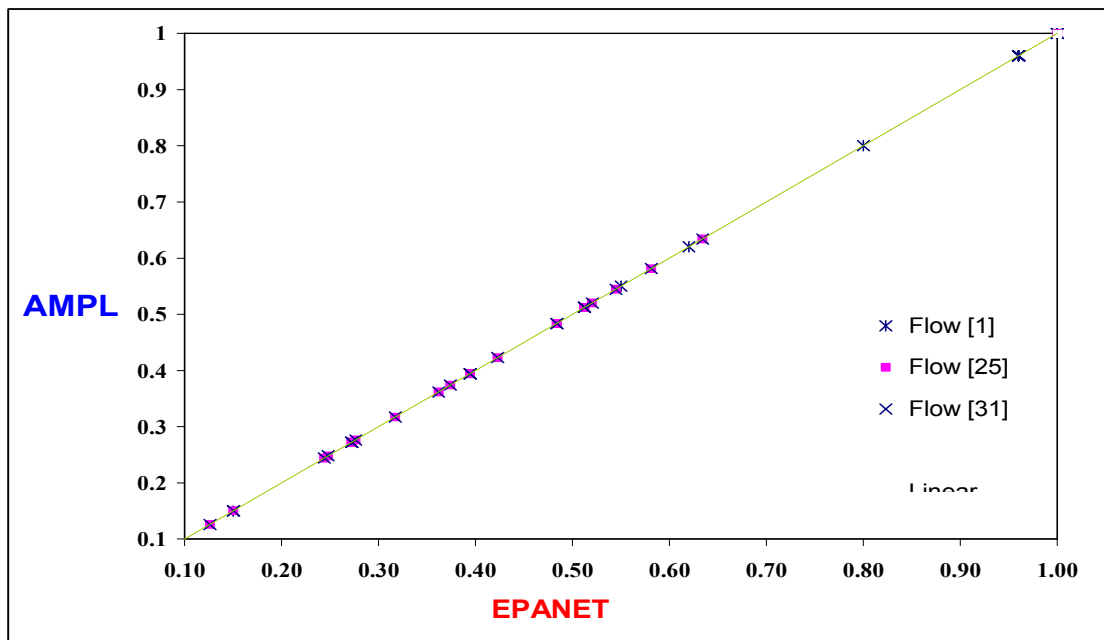


Figure 5-11: Normalized Flow in Links (1, 25 and 31) in Case Study 2

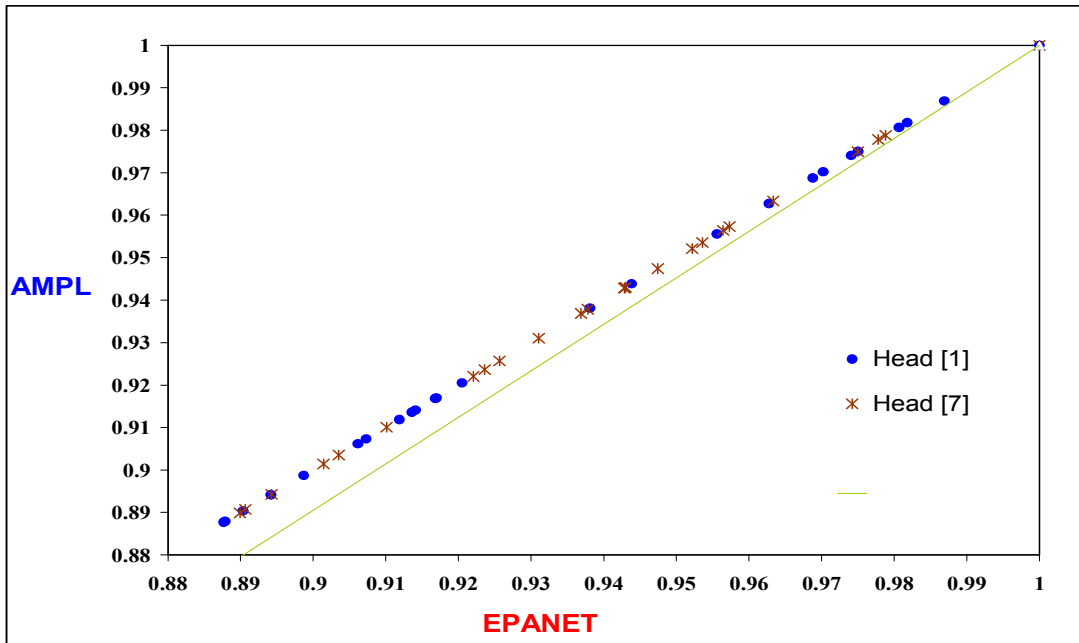


Figure 5-12: Normalized Head at Nodes (1, and 7) in Case Study 2

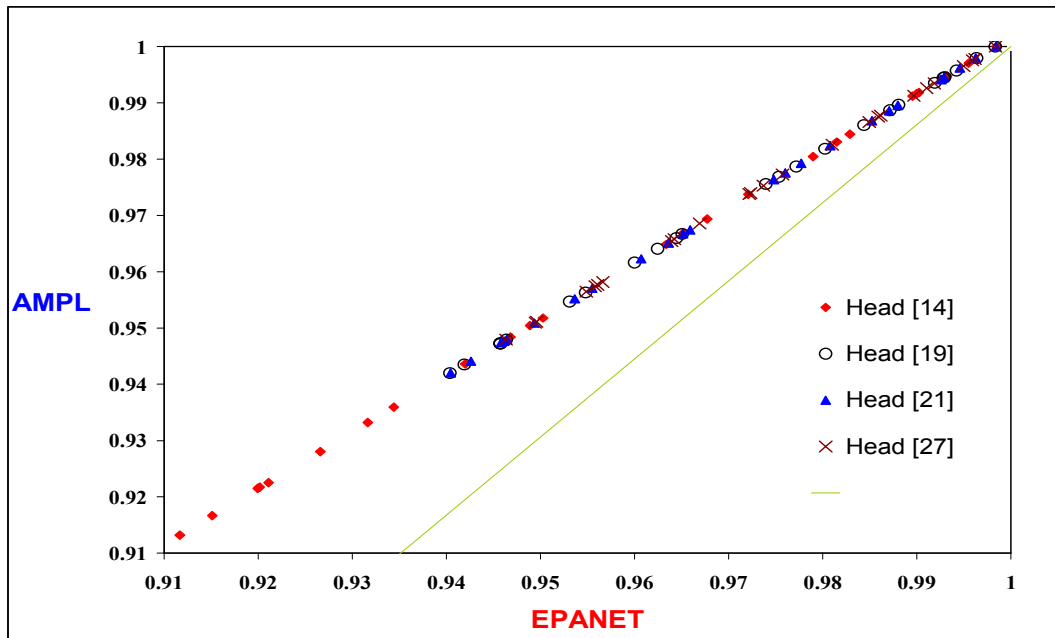


Figure 5-13: Normalized Head at Nodes (14, 19, 21, and 27) in Case Study 2

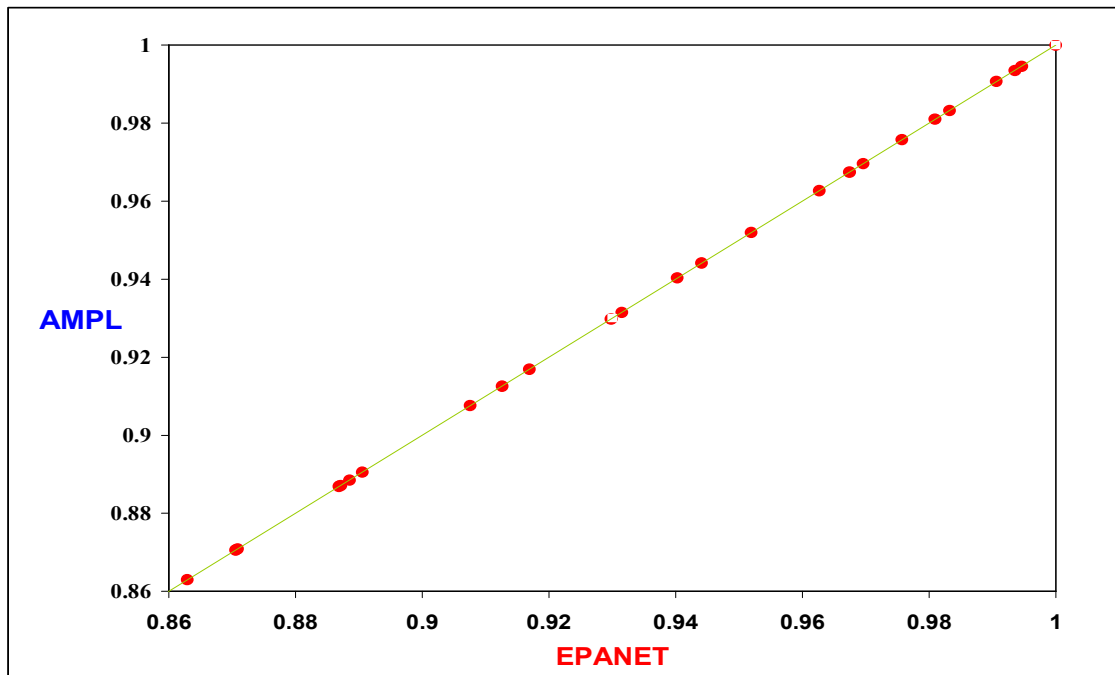


Figure 5-14: Normalized Level in Tank (26) in Case Study 2

### 5.3.3 Validation Results for Case Study 3

Finally for Network3 and to demonstrate the level of matching between the AMPL model and EPANET, values of selected flows in Links (251, 277, 111, 171, and 241) as well as head pressure at Nodes (101, 121, 145, 197, 157, 265, 199, 219, and 237) are compared graphically as before in Figures 5-15 through 5-19. Water level in the three Tanks is shown in Figure 5-20.

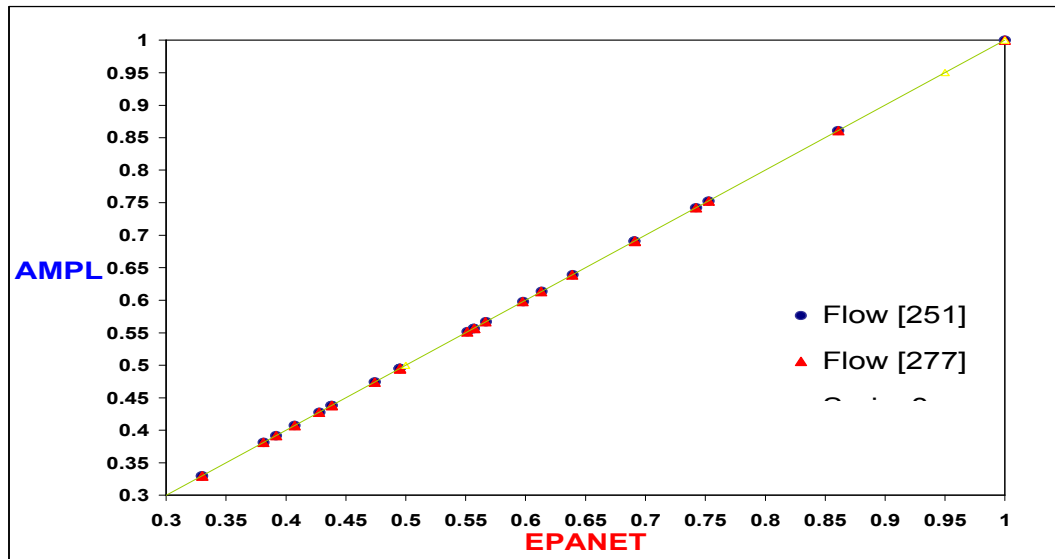


Figure 5-15: Normalized Flow in Links (251, 277) in Case Study 3

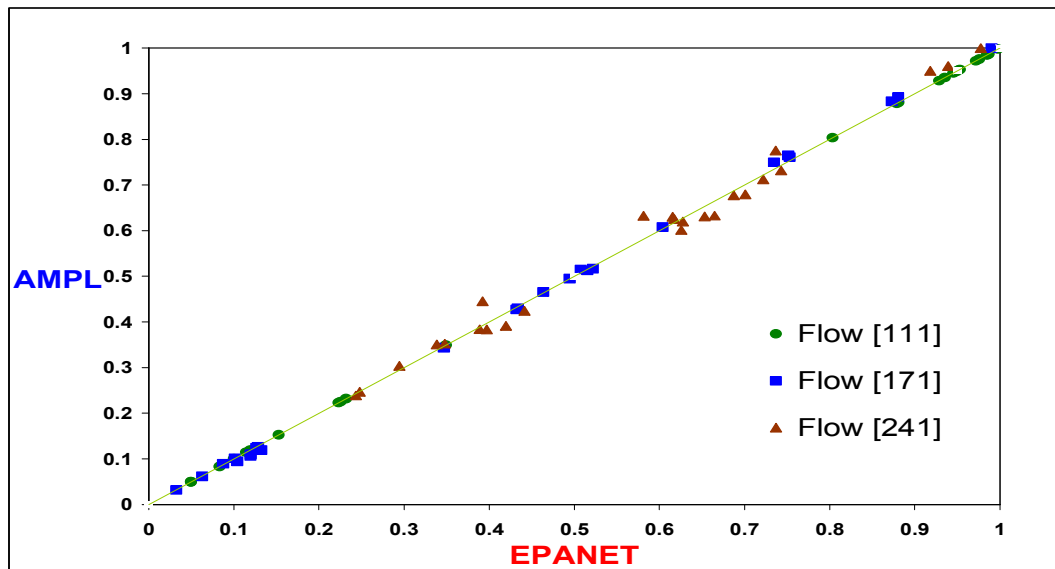


Figure 5-16: Normalized Flow in Links (111, 171, and 241) in Case Study 3

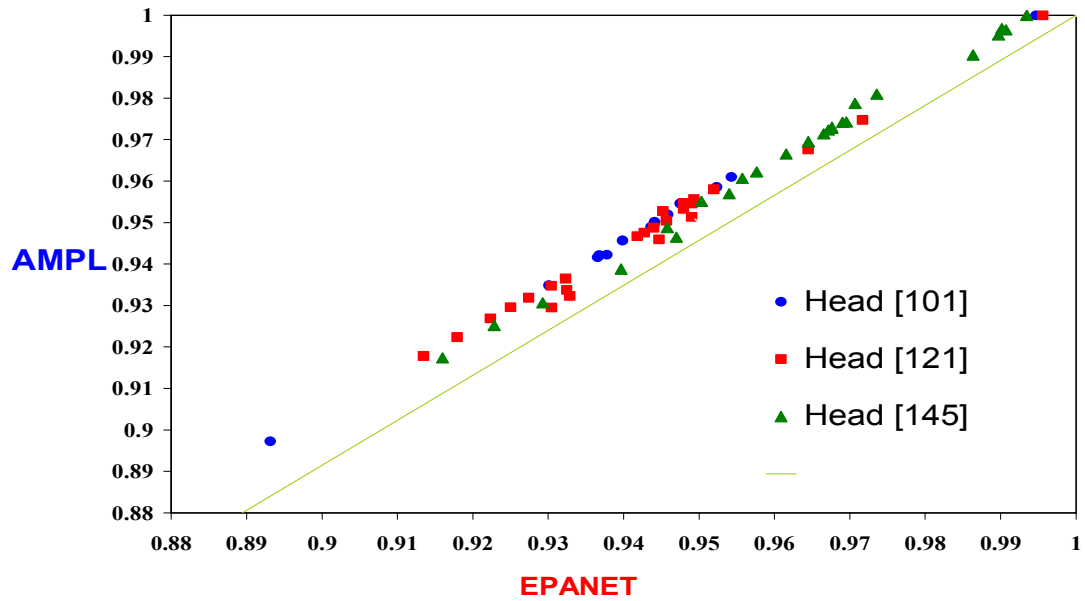


Figure 5-17: Normalized Head at Nodes (101, 121, and 145) in Case Study 3

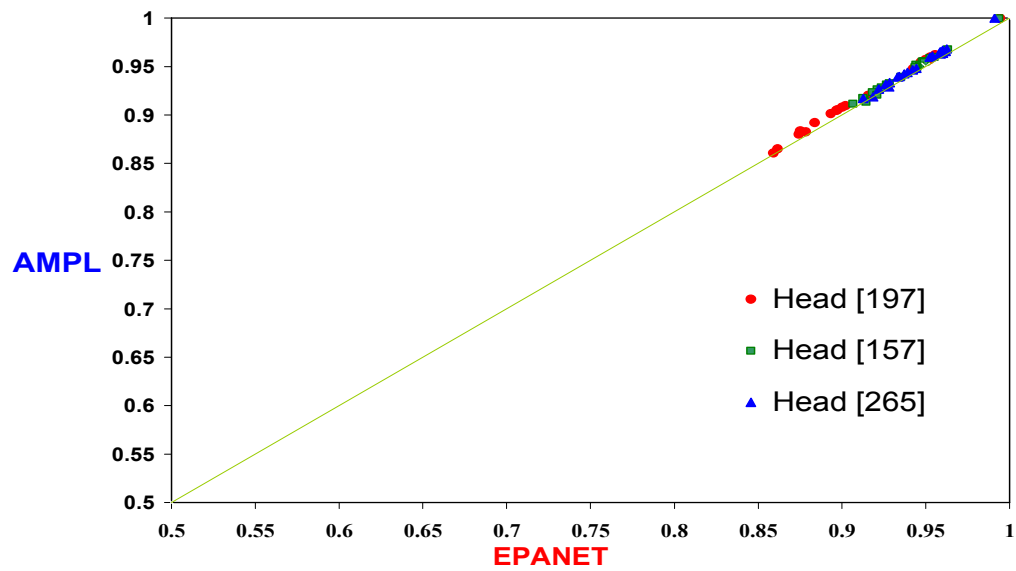


Figure 5-18: Normalized Head at Nodes (179, 157, and 265) in Case Study 3

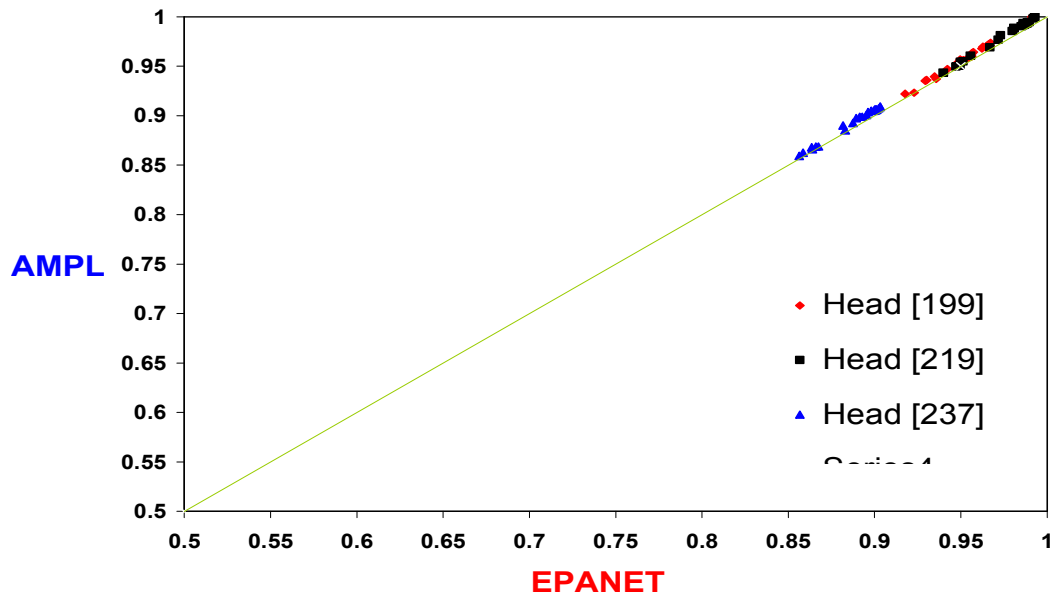


Figure 5-19: Normalized Head at Nodes (199, 219, and 237) in Case Study 3

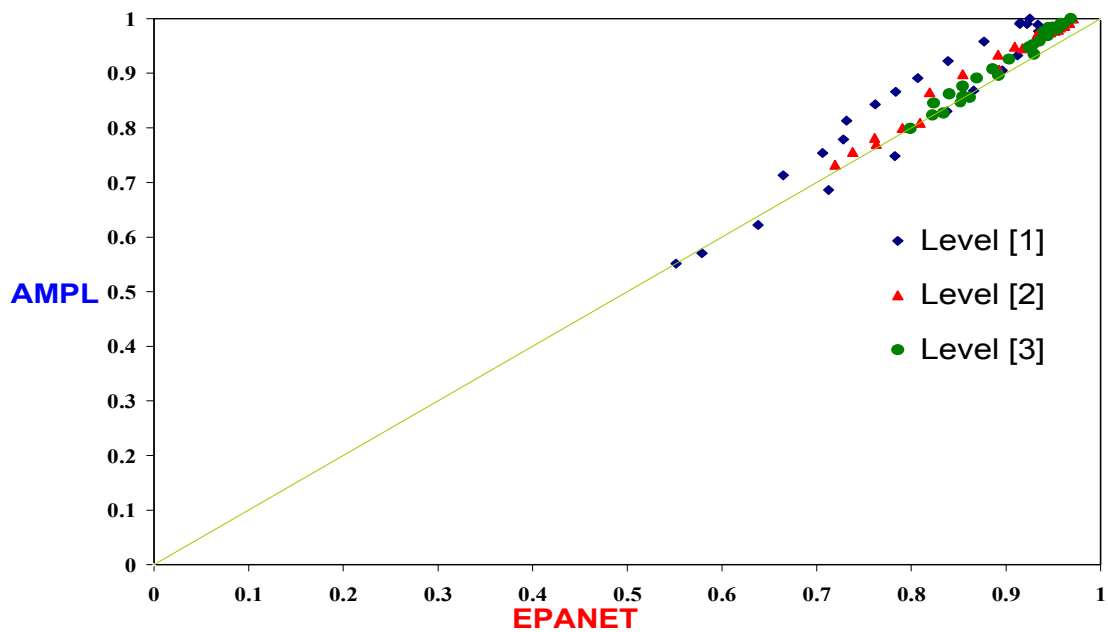


Figure 5-20: Normalized Level in Tanks (1, 2, and 3) in Case Study 3

## CHAPTER VI

### RESULTS AND DISCUSSION

In Chapter IV and V the optimization formulation was described and the model was validated. Here, the full estimation problem with different sensors layouts is considered using the three case studies that were previously described in Chapter V. The formulation is tested for its ability to determine flows and pressures in the system from limited measurements data.

Figure 6-1 describes the process used to test the formulation for a given case study and sensor layout. EPANET is used first to simulate the true system. The true demands are given as input to EPANET and the flow and the pressures are calculated. A subset of these results is fed to the optimization formulation representing the available measurements. The optimization formulation is also given the assumed demands based on historical estimates. The optimization formulation is solved for the estimated demands, flows, and pressures which are then compared with those obtained from EPANET.

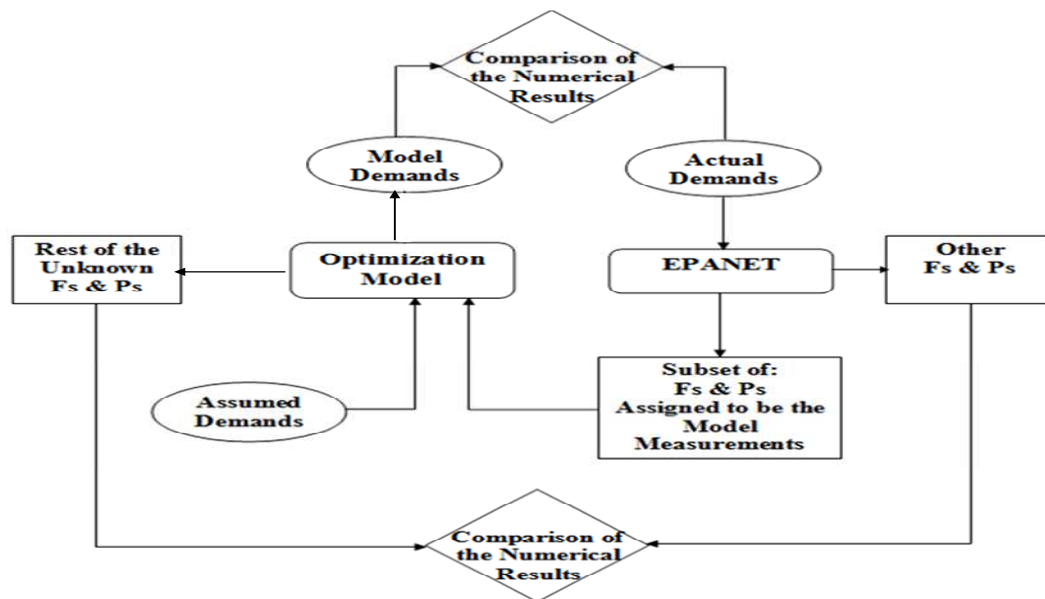


Figure 6-1: A Schematic Diagram for the Real Problem



With this testing procedure, two questions need to be answered. First, how are the true and the assumed demands set. Second, how will the location of the measurements be selected. Here, the true demands are those demand patterns obtained from EPANET and represent the input data for the simulator when solving each one of the three selected case studies. The assumed demands are generated by the addition of noises to the demand patterns in the EPANET case studies. These noises are generated by introducing a normal distribution function that uses the EPANET demands as the mean values and assumes different values for the standard deviation. This tests the effectiveness of the model to estimate the real demands when large deviation in the offline demand estimates exist. The second concern is the selection of measurements. The formulation will be tested using different sensor configurations. Here, only the selection of flow sensors is considered, however future work can include both flow and pressure measurements.

The optimization problem is coded in the mathematical programming language AMPL. AMPL was first introduced in 1993 as an optimization tool for linear and non-linear programming. It is notable for the similarity of its arithmetic expressions to customary algebraic notation. A flexible interface allows the user to choose from different types of solvers to improve the solver performance (Fourer et al. 2003). In the current work, all problems are solved using the nonlinear interior-point solver (IPOPT), (Wachter 2002).

## **6.1 Selecting Flow Measurements**

The degrees of freedom for a system of equations describing a water network are determined by the number of junctions with non-zero demands as shown before in section 4.3. In simulation, the degrees of freedom are usually satisfied by specifying the demand pattern at each junction. When the set of the demands is given, the problem is totally defined and the resulting system of non-linear equations can then be solved for pressures and flows. However, if pipe flow rates are given, only subset of the network pipes is necessary to satisfy the degrees of freedom. Therefore, when limited numbers of flow sensors are available, it is important to ensure that they are not redundant. A graph theoretical approach is adopted from Rahal (1995) to determine the non-redundant set of

flow measurements that satisfy the degrees of freedom. Then, the tests are performed using limited number of sensors from this set. The graph theory approach is briefly described in the following section. More information about graph theory and its applications can be found in the following references (Bondy and Murty 1967; Bang-jensen and Gutin 2000; and Diestel 2005).

### 6.1.1 Fundamentals of Graph Theory

A graph is a pair of  $(V(G), E(G))$  where  $V(G)$  is nonempty set of vertices (nodes) and  $E(G)$  is a set of edges (links) connecting the vertices together. A graph can be classified as directed or undirected, cyclic or acyclic, and connected and disconnected. Figure 6-2 shows an example of these graphs. The following terminologies are also important.

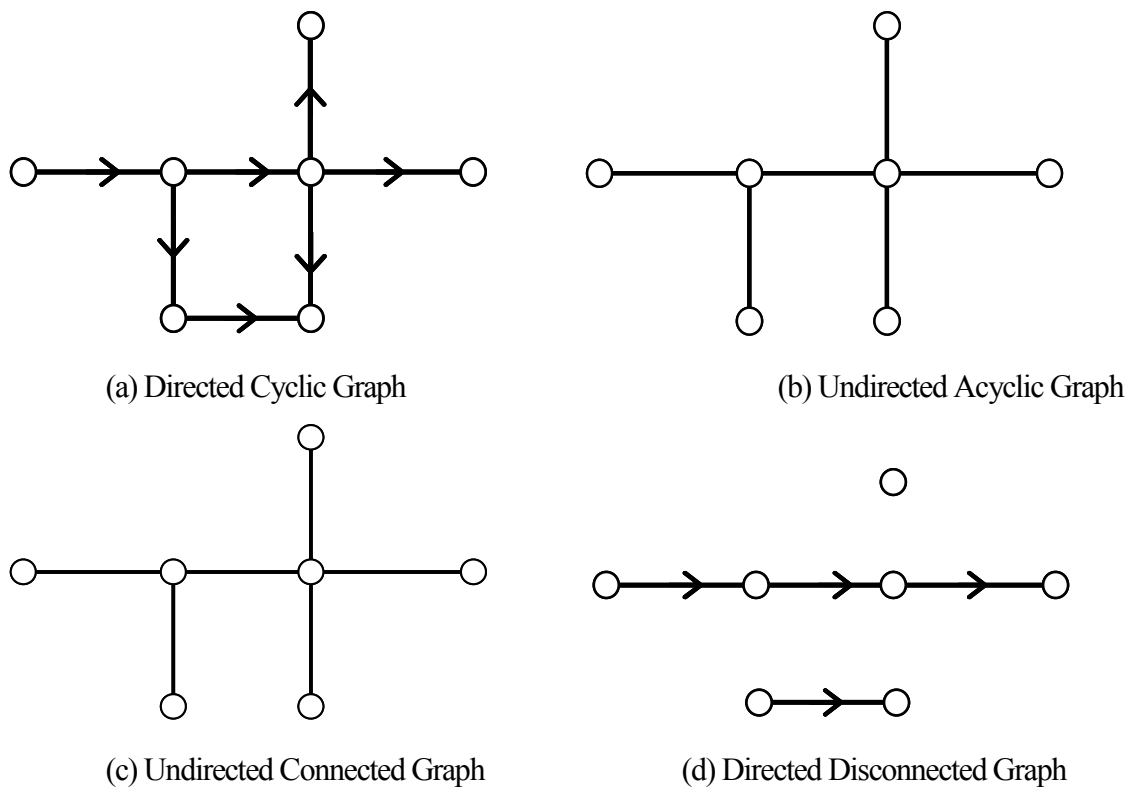


Figure 6-2: (a) Directed Cyclic; (b) Undirected Acyclic; (c) Undirected Connected; (d) Directed Disconnected Graph

*Tree T.* A tree T of graph G is a non-cyclic subgraph with all nodes being connected such that a unique edge links any two nodes together. Graph theory states that for any graph G with n-nodes, the number of links of any tree T with respect to this graph is (n-1) links. The links of any tree T are called branches. Figure 6-3 shows all possible trees for a six-node graph.

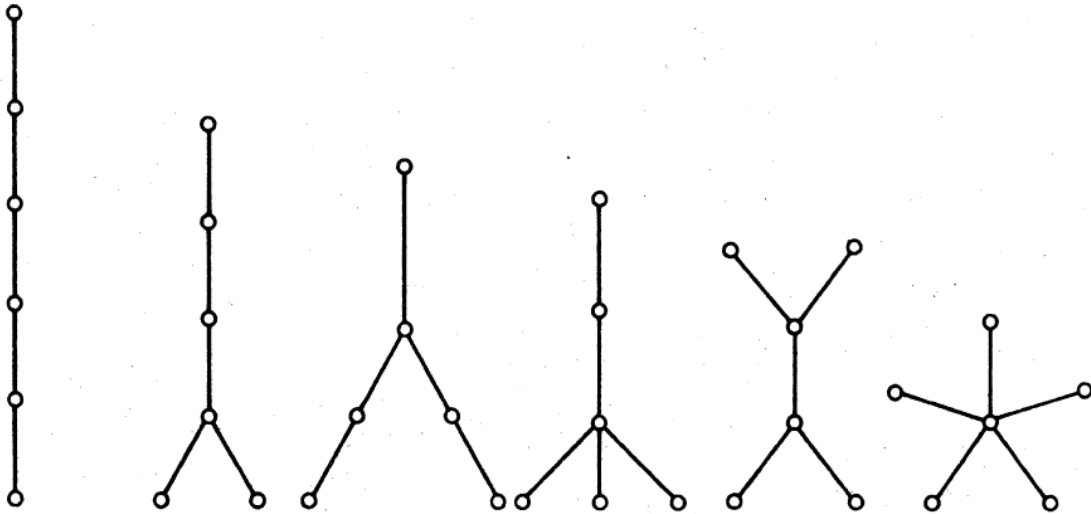


Figure 6-3: All Possible Trees on a Graph with Six Nodes.(Bondy and Munty 1967)

*Co-Tree  $\bar{T}$ .* A co-Tree is the complement with respect to tree T. Union of tree T and its complement co-tree T forms the origin graph G. The co-tree links are called chords. The number of chords can be determined by subtracting the number of links in the corresponding tree (n-1) from the total number of links (P) in the graph as follows:

$$\begin{aligned} \text{Number of chords} &= P - (n-1) \\ &= P - n + 1 \end{aligned} \quad (6-1)$$

*The Cyclomatic Number ( $n_L$ ).* Because the tree does not have loops or circuits, it is obvious that adding any of the chords to the tree T will create a cycle (r). Hence, the number of cycles (loops) will be the same as the number of the chord links (P- n + 1).

$$\text{Number of loops, } n_L = \text{Number of chord links} = P - n + 1 \quad (6-2)$$

*Circuit (loop) Matrix C.* In any connected graph, there are  $(n_L)$  of fundamental loops. The circuit is said to be fundamental if it has at least one unique link which does not exist in any other loop. The matrix  $C$  ( $n_L \times P$ ) defines the link  $j$  that belongs to specific loop  $i$ . Thus, the element  $c_{ij}$  can be defined as follows:

$$c_{ij} = \begin{cases} 1, & \text{if link } j \text{ exists in loop } i \text{ and has the same direction of the loop} \\ -1, & \text{if link } j \text{ exists in loop } i \text{ but has the opposite direction of loop } i \\ 0, & \text{if link } j \text{ does not exist in loop } i \end{cases}$$

The direction of a circuit is determined by the direction of the unique co-tree chord that belongs to this circuit.

*Cut-set Matrix K.* Because the tree represents the minimum number of links that connect all the nodes together without creating loops, whereas the cut-set is the set of the links that disconnect some nodes from the origin graph, any tree –sometimes refers to as spanning tree- must have at least one link in common with one of the cut-sets associated with the corresponding graph. The number of the cut-sets  $n_k$  is defined as  $(n-1)$ . The matrix  $K$  ( $n_k \times P$ ) identifies which links belong to specific cut-set, Thus the element  $k_{ij}$  can be determined as follows:

$$k_{ij} = \begin{cases} 1, & \text{if link } j \text{ exists cut-set } i \text{ and has the same direction of the cut-set} \\ -1, & \text{if link } j \text{ exists in cut-set } i \text{ but has the opposite direction of the cut-set} \\ 0, & \text{if link } j \text{ does not exist in cut-set } i \end{cases}$$

The direction of a cut-set is determined by the direction of the unique branch of the spanning tree.

*Network Flow and Potential.* Water network forms a digraph (or a directed graph) where some nodes have high potential (head) which are called sources and other nodes that have low potential which are called sinks. Due to the difference in potential, a flow (discharge) is going from a source to a sink. Both the potential difference vector  $\Delta H^T = [\Delta h_1, \Delta h_2, \dots]$  and the flow vector  $F^T = [F_1, F_2, \dots]$  are governed by Kirchhoff laws:

$$K F = 0 \quad (6-3)$$

$$C H = 0 \quad (6-4)$$

As discussed earlier in section (3.2.2), Hazen-William formula was selected to express the head losses in links. Following the matrix notation used here, the head losses matrix can be written as a function of the flow matrix as follows:

$$\Delta H (F) = R F^a \quad (6-5)$$

Where R is a diagonal resistance matrix formed from Equation (3-10) that includes the link diameter, the link length and the roughness coefficient.

*Chord Link and Branch Link Flows.* Based on Equations (6-3) through (6-5), the resulting governing system of equations describing the network can be represented as:

$$\left\{ \begin{array}{ll} K F = 0 & : (n-1) \text{ cut-set equations} \\ C H = 0 & : (P-n+1) \text{ loop equations} \\ \Delta H (F) = R F^a & : (P) \text{ resistance equations} \end{array} \right.$$

### 6.1.2 Chord Flow Decomposition Method

The system of Equations (6-3) to (6-5) has (2P) equations and (2P) variables; the link Flow (F) and the head losses variable (H). Rahal (1995) introduced a decomposition approach using the graph theory principles to reformulate the problem in fewer equations. The new system of equation is expressed as a function of the flows in the chord links (the co-tree links) only, (Rahal 1995). The network shown in Figure 6-4 will be used to illustrate this method and how it is applied.

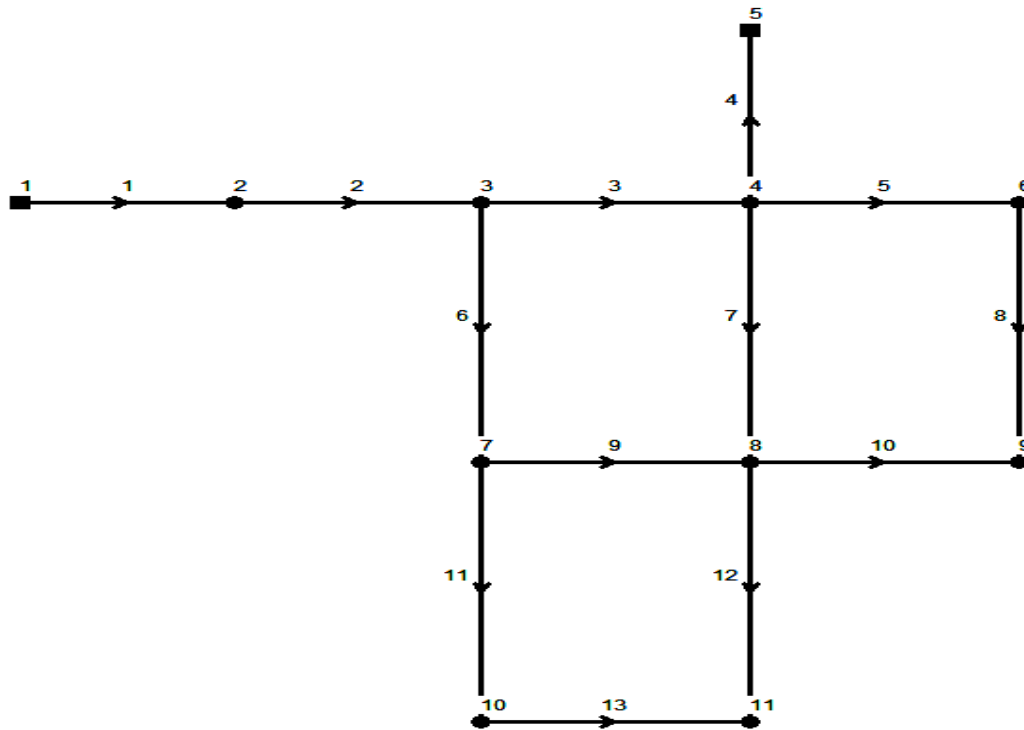


Figure 6-4: Illustrative Example Network

Step 1:

The network is first represented as a circulating graph in which the demand assigned for a specific node is represented by a pseudo-link that joins this node to source node in the graph. For instance, re-representing the network shown in Figure 6-4 should have a pseudo link going from each node to node (1) and carrying the demand value as pseudo flow. Figure 6-5 shows the modified network after adding the pseudo demand links.

Step 2: Identifying a Spanning Tree

The spanning tree is the set of links that connect all the  $n$ -nodes together without creating loops. The  $(n-1)$  links belonging to this set are called branches. The complement set of  $P - (n-1)$  links are called the chord links, where  $P$  is total number of links in the system. For the network shown in Figure 6-3 with 11 nodes and 13 links, there will be 10 branches and 3 chords. There are different possible spanning trees and here, links 5, 6, and 12 are selected as the chord links. The branches and

the chords are shown in Figure 6-5 in which the branches are the thick lines and the chords are the slim ones.

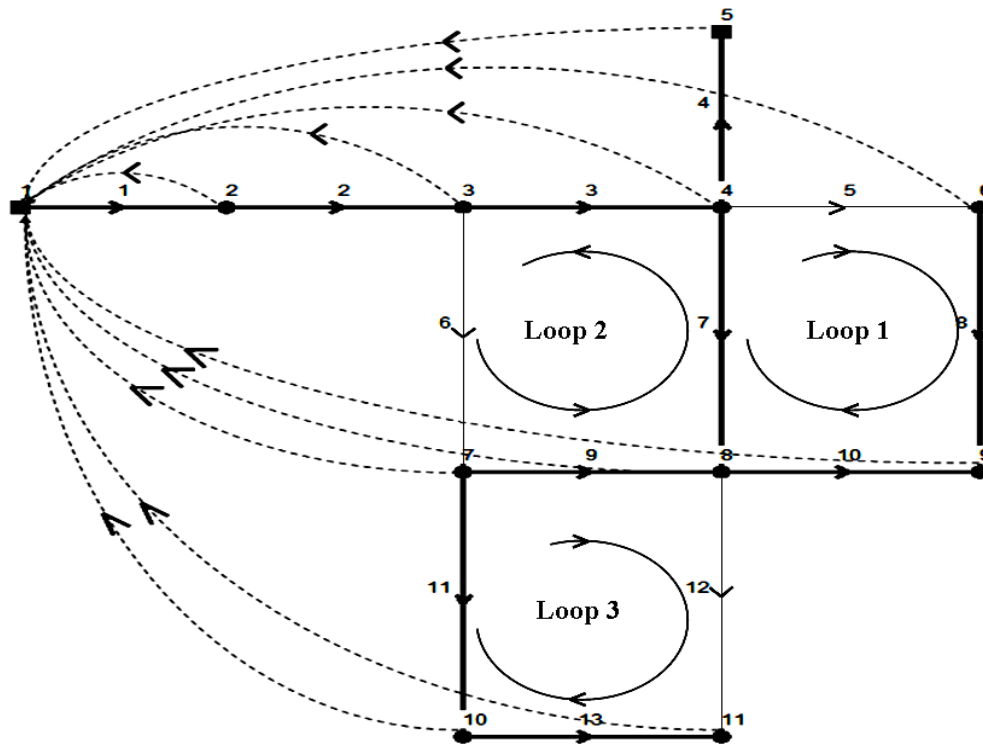


Figure 6-5: Pseudo Demand Links, Branches, and Chords in the Example Network

Rahal (1995) outlined a decomposition approach for simulation to reduce the number of equations necessary to describe the system. The resulting system of equations can be expressed as a function of the tree flows only which was shown to have the same dimension as the demands and hence the degrees of freedom. Therefore, specifying  $(n-1)$  tree flows is sufficient to satisfy the degrees of freedom and hence the problem can be solved to determine the unknown “Chord Flows”, pressures, head losses, and demands. This number of specification is consistent with the  $(n)$  degrees of freedom of the main problem described in section (4-3). The one-difference in the two numbers can be explained by noting that in the current model the demand set was defined over all the nodes (junctions and sources), whereas the demands in Rahal method were defined only for the junctions.(i.e. excluding the water source).

The discussion mentioned above suggests that measurements should always be kept on the set of the “Tree Flows”. In practice, fewer flow measurements will be available. While more measurements can be used to reduce the non-uniqueness in the estimation problem, they must be selected in such a way that they are not redundant. To ensure this, different sensor configurations are to be randomly selected from the tree flows only.

## 6.2 Case Studies

The following sections show the effectiveness of the estimation formulation when the number of measurements on the tree flow set varies from very few measurements up to the total number of the degrees of freedom, (n-1). The method will be applied for the three case studies: Case Study 1, Case Study 2, and Case Study 3

To determine the estimation accuracy, the following expressions are used to express the percentage error in flow in link k at time j as the difference between the calculated flow from the model and the flow from the simulator EPANET which represent the true flow divided by the true flow. This can be formulated as follows:

$$e_F(k, j) = \frac{|F(k, j) - SF(k, j)|}{|SF(k, j)|} \times 100 \% \quad (6-6)$$

The time-averaged error of flow per link is the summation the basic error  $e_F(k, j)$  described in equation (6-20) over the whole simulation period (t) as follows:

$$E_F(k) = \frac{1}{t} \sum_{j=1}^t e_F(k, j), \forall k \quad (6-7)$$

The overall error in flow in the network for specific scenario can be obtained by summing the time-averaged error in each link over the whole set of links which aims to compare different scenarios based on a single measure.

$$E_F = \frac{1}{P} \sum_{k=1}^P E_F(k) \quad (6-8)$$





As mentioned earlier, the deviations in demands are generated by the addition of noises to the demand patterns from the EPANET. These noises are generated by introducing a normal distribution function that uses the EPANET demands as the mean values and tests different values for the standard deviation. Figure 6-7 shows the overall error in flows for each proposed scenario assuming 0.1 standard deviation in the demand distribution function. At 3 measurements, the overall error in flows reaches only 1.2%. Increasing the number of measurements from 1 to 3 measurements reduce the overall error in flows by 9.3%, while increasing the number of measurements further only reduce overall error slightly to 0.09% with all 10 measurements

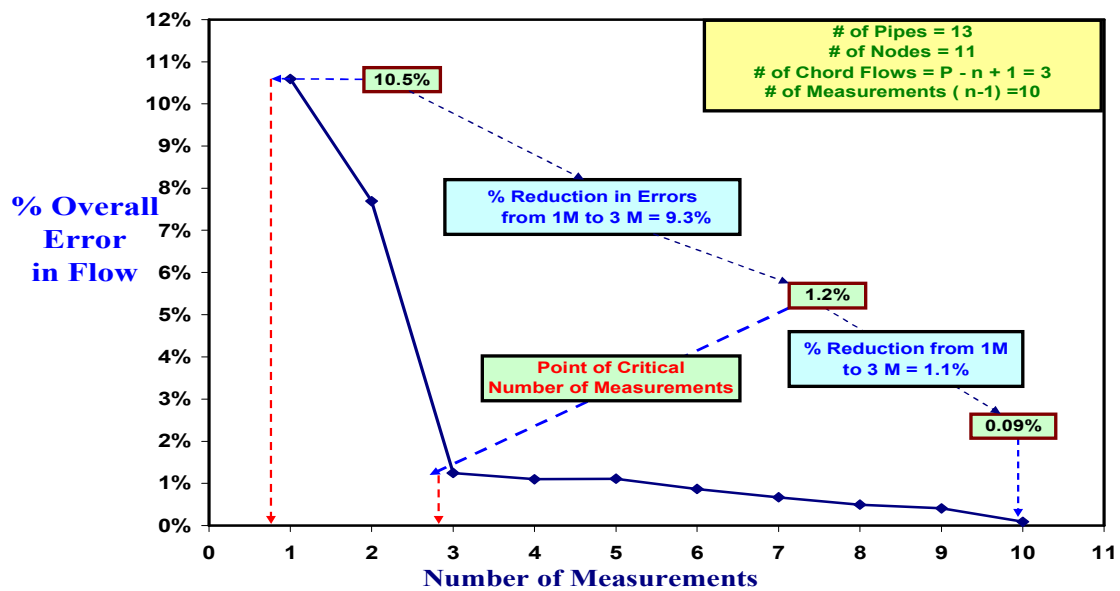


Figure 6-7: % Error in Flow in Network1 with 0.1 Standard of Deviation in the Offline Demand Function

Figure 6-8 shows the results for four different values of the standard deviation in the demand distribution function; (0.01, 0.05, 0.1, and 0.5). In each of these cases, it is interesting to note that a number of three measurements appears to be a critical number.

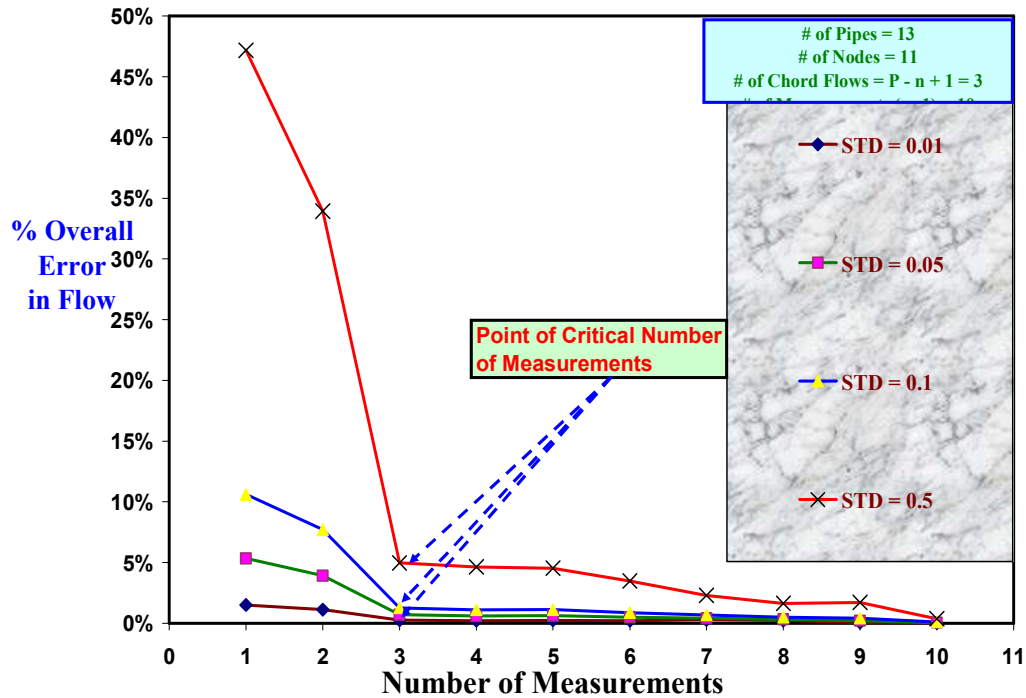


Figure 6-8: % Error in Flow in Case Study 1 with Different Standards of Deviation in the Offline Demand Function

Preliminary results suggest that changing the selection of measurements or selecting different tree and chord links do not appear to change this critical number. Figure 6-9 shows a different configuration for placing measurements by selecting links {12, 111, and 122} as new chord links. Figure 6-10 shows a similar behavior as the previous configuration when selecting {31, 111, and 113} as chord links. It is clear that both figures still point to 3 as a critical number of measurements.

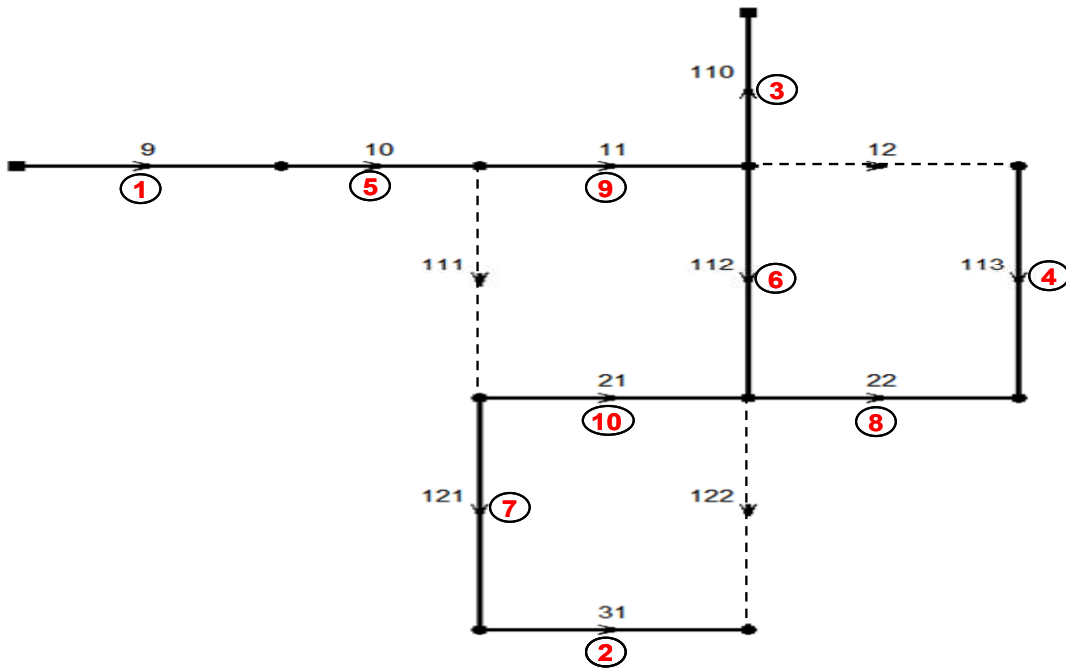


Figure 6-9: Chord and Tree Links and Sequence of Adding Measurements in Case Study 1, Configuration 2

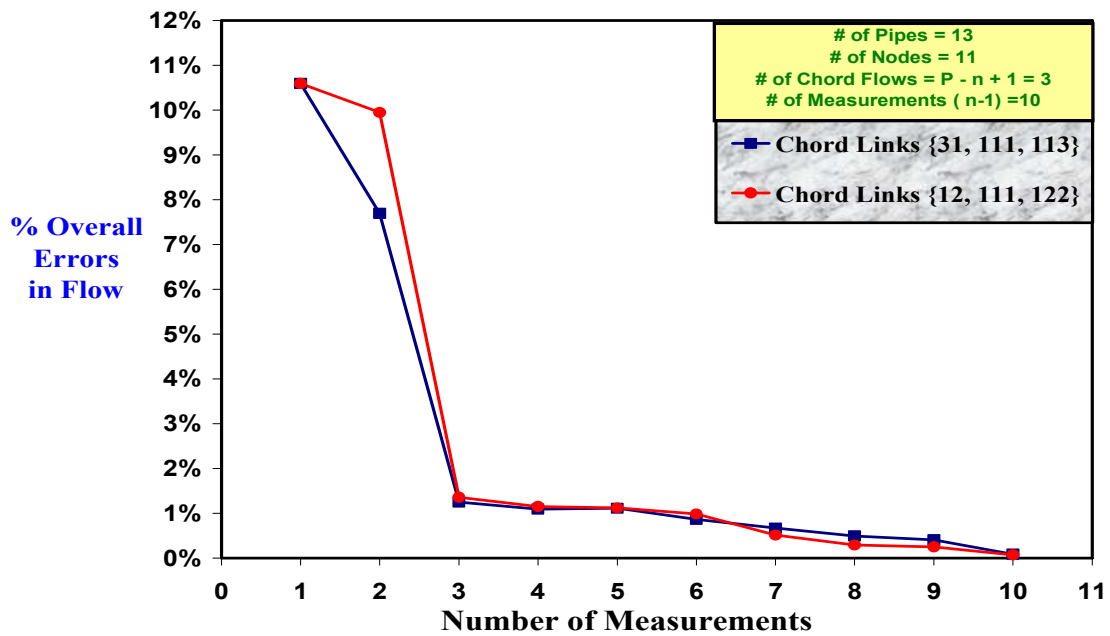


Figure 6-10: % Error in Flow in Case Study 1 for Two Measurements Configuration

## 6.2.2 Case Study 2

As shown in Figure 6-11, Case Study 2 consists of 36 nodes and 40 links which, based on Equation (6-2), requires identification of 5 different chord links. The remaining 35 links will represent the full set of measurements required to completely define the problem.

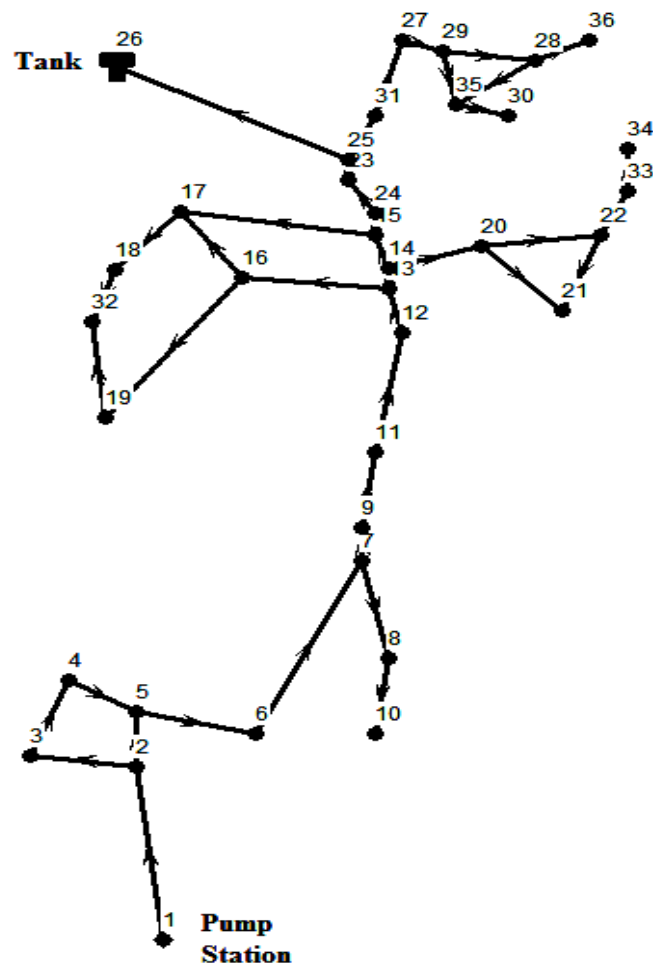


Figure 6-11: A Schematic Diagram for Case Study 2

For small networks or networks with less interconnectivity in links, different spanning trees can be determined easily by hand. However in large and heavily interconnected networks, another approach is required. A planar graph is a graph in which the links are connected only in nodes.

One approach suggests representing any graph in its equivalent planar graph and, in addition, drawing the network in a tree-like structure with placing a loop on one side of the main tree branch. For middle-size networks, this approach can help determine the fundamental loops and one possible spanning tree with its associated chords. Figure 6-12 shows a different representation for the network in Case Study 2 in a planar tree-like structure. It is easy to determine the 5 different fundamental loops. From the definition of the chord links it is clear that by removing a unique link from each fundamental loop, one possible spanning tree is formed. The chord links are represented in Figure 6-12 by dotted and slim lines, while the tree branches are represented by the solid and the thick ones.

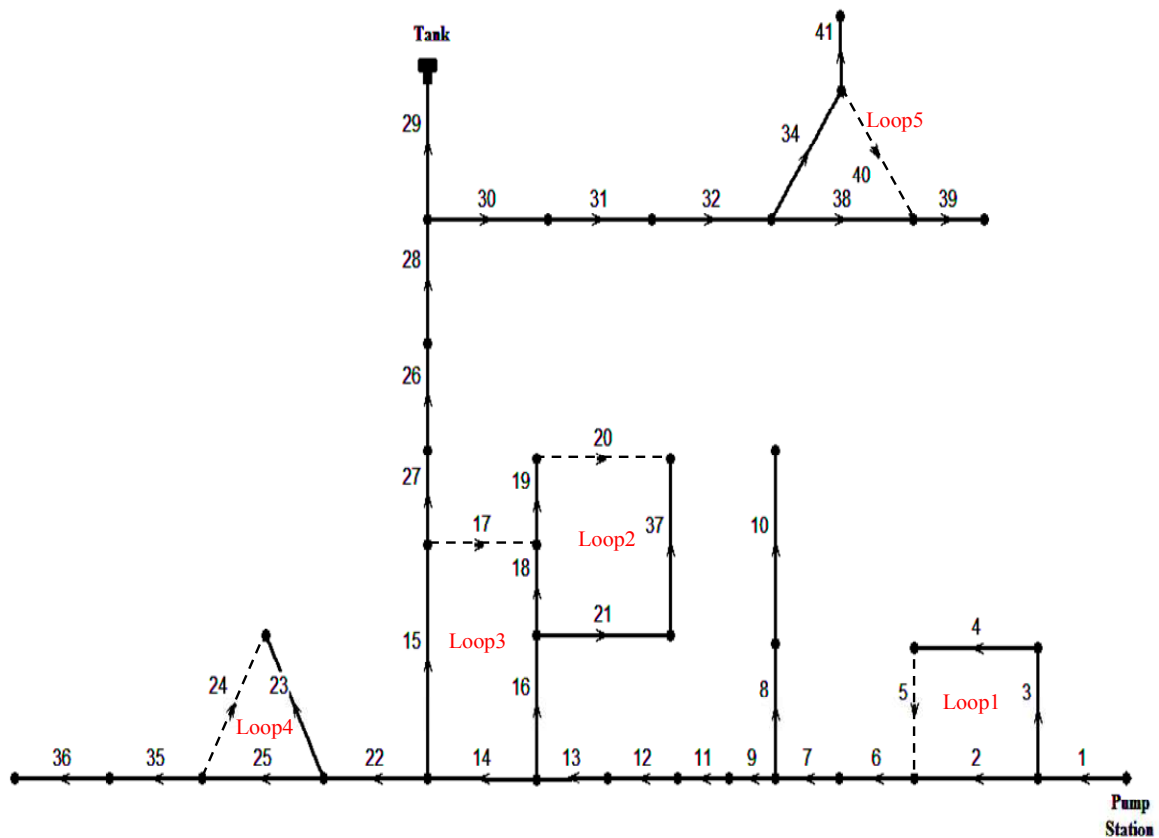


Figure 6-12: Planar Graph for Case Study 2 with One Possible Configuration for the Chord and the Tree Links

Based on this approach, links {5, 17, 20, 24, and 40} are considered as the chord links and the remaining links as the full set of measurements. Ten different scenarios are investigated with the number of measurements being increased in each successive scenario. Figure 6-13 show the overall error as a function of the number of measurements in each scenario. Similar to the previous case study, there is a critical number of measurements at which the overall error in estimating the flow is reduced significantly. For Case Study 2, two jumps occur at 4 and 15 measurements. Figure 6-14 shows the overall error for different values for the standard deviation in the demand distribution function.

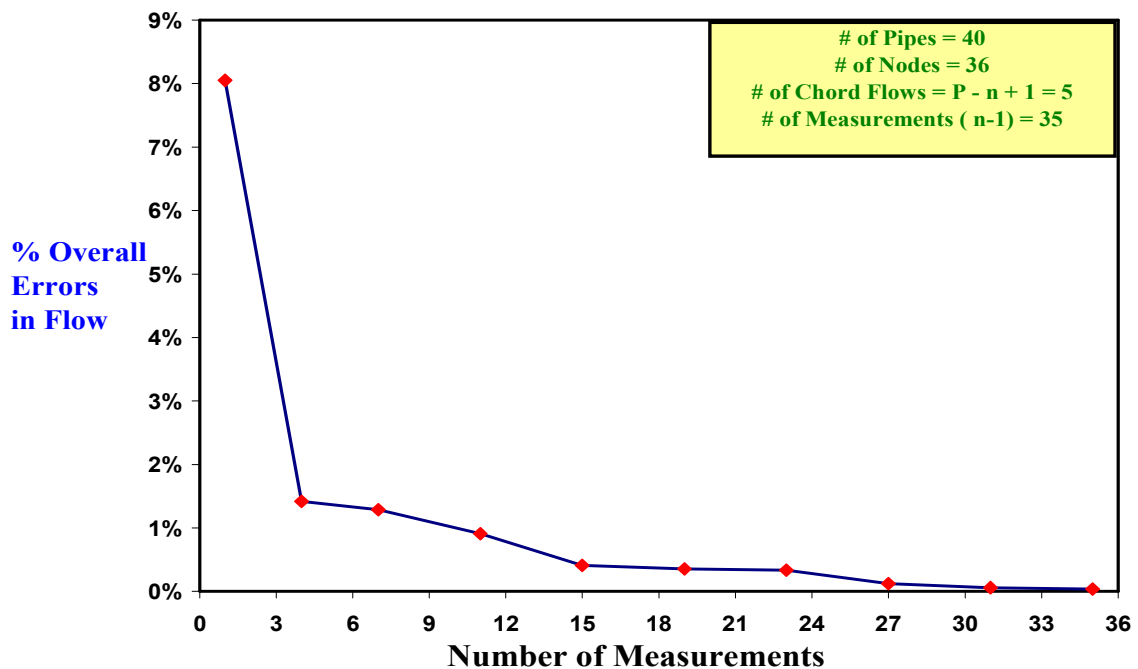


Figure 6-13: % Error in Flow in Case Study 2 with 0.1 Standard of Deviation in the Offline Demand Function

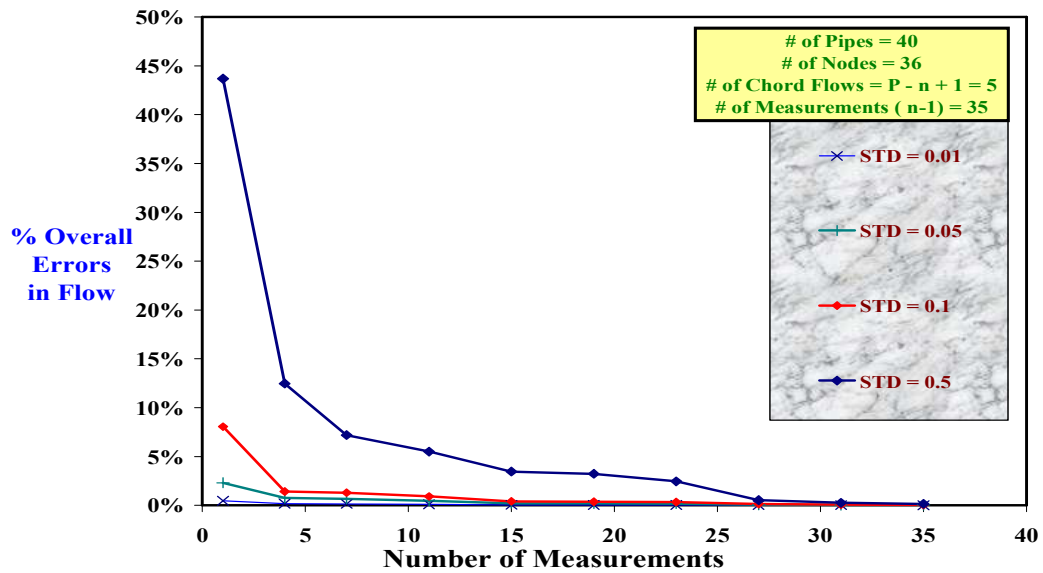


Figure 6-14: % Error in Flow in Case Study 2 with Different Standards of Deviation in the Offline Demand Function

### 6.2.3 Case Study 3

The third and the largest case study consists of 96 nodes and 117 links as shown in Figure 6-15. It is difficult for large-size networks such as Case Study 3 to determine the spanning tree by the hand. Two methods based on tree-searching algorithm can be used; the depth-first search and the breadth-first search.

The depth-first method begins by selecting an arbitrary starting node which is labeled as “root” node. This node is then marked as being “visited”. Next, a direction is chosen to the right or the left to one of the adjacent (connected) nodes to the root and the selected node is also marked as being “visited”. The selected node becomes the new root and another downward direction to an adjacent node is selected. The search continues until there is no more possible movement. From the last node reached in this branch, a step is taken back to the previous node searching for other possible



directions. If there is another possible direction, it is taken downward and a new branch is created. The process is continued till all the nodes are visited.

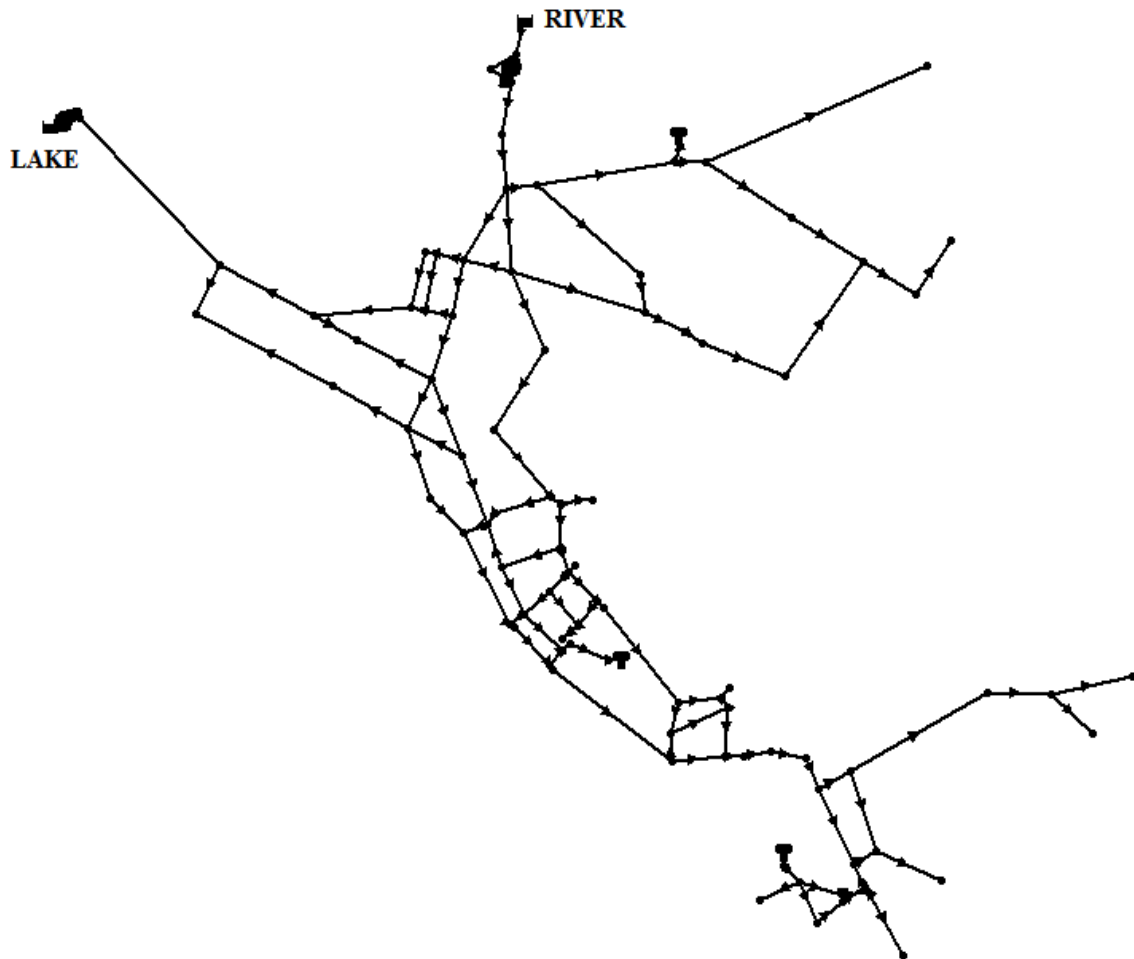


Figure 6-15: A Schematic Diagram for Case Study 3

In the breadth-first search, an arbitrary node is also selected and labeled as “root” node. The node is marked as being visited. Next and unlike the depth-first method, all the possible direction to the set of the adjacent nodes to the root node is considered and the reached nodes are marked as being visited. The set of the connected nodes to the root node represent the first level of search. From this level, one node is selected to be the new root and all possible directions to the connected nodes to the new root node are considered. The procedure is repeated till there is no more

movements to other connected nodes. A step is taken back to the first intersection passed and a new branch is created from this node in the same fashion till all the nodes are visited. Figure 6-16 shows an illustrative example of one possible tree and the resulting network when the depth-first is applied for the original network shown in Figure 6-1, while Figure 6-17 shows the tree and the network resulting from the application of the breadth-first method for the same origin network.

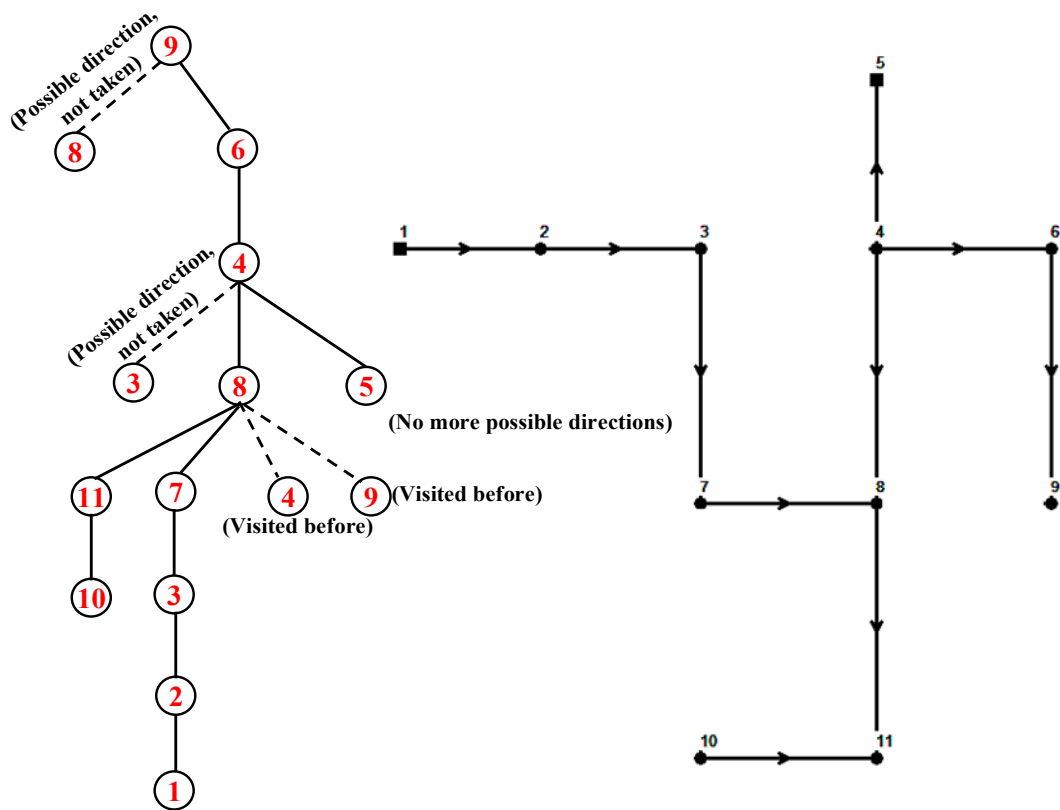


Figure 6-16: The Depth-First Search and The Resulting Tree for the Network  
Shown in Figure 6-3

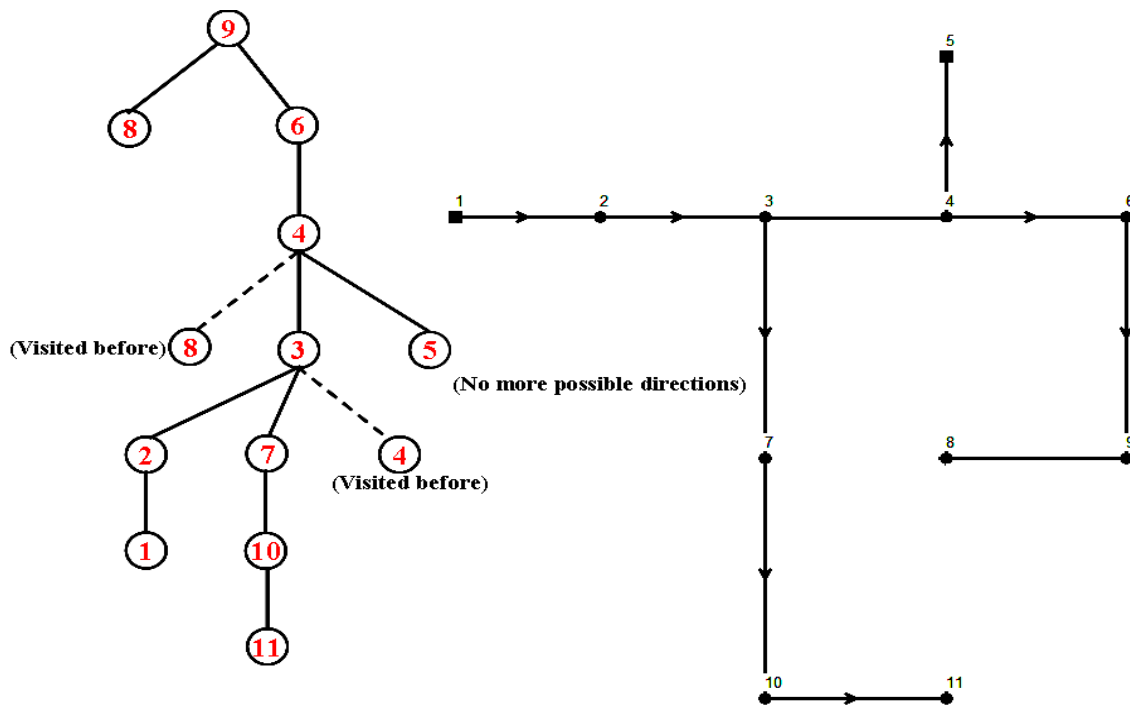


Figure 6-17: The Breadth-First Search and the Resulting Tree for the Network  
Shown in Figure 6-3

As default algorithm, the depth- first search method is implemented in MATLAB library and it is used to determine different possible spanning trees for Case Study 3. For a network with 96 nodes and 117 links, the number of chords is 22 and the remaining 95 links form the set of the spanning tree. MATLAB was used to determine different possible spanning trees. 19 different scenarios were investigated. The first scenario uses only five measurements, while the number of measurements is increased equally by adding additional five measurements in each following scenario.

Figure 6-18 shows the overall error in flows against the number of measurements for 0.1 standard of deviation in the demand assumption distribution function. The figure shows a region near 40 measurements in which the overall error can be reduced significantly. The effect of different standard deviations in the demand distribution function is shown in Figure 6-19. The figure shows similar profile for each scenario.

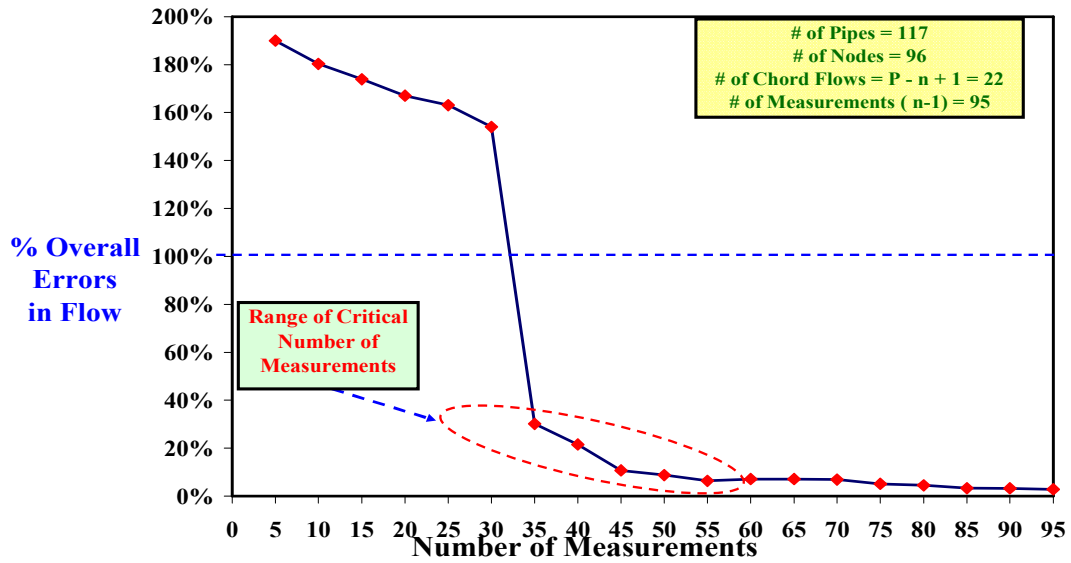


Figure 6-18: % Error in Flow in Case Study 3 with 0.1 Standard of Deviation in the Offline Demand Function

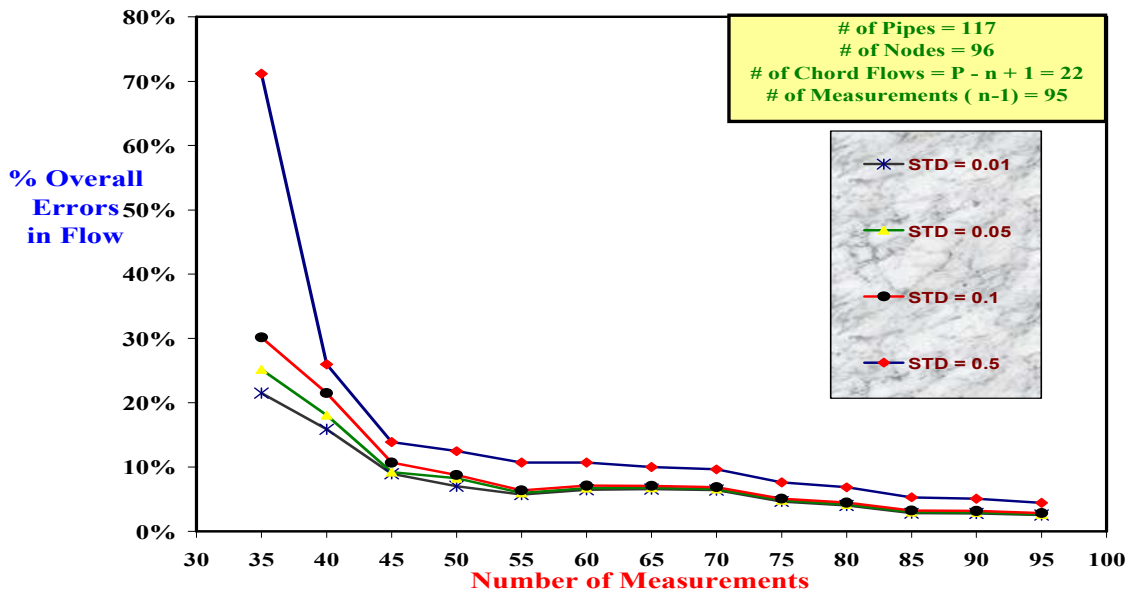


Figure 6-19: % Error in Flow in Case Study 3 with Different Standards of Deviation in the Offline Demand Function

## **CHAPTER VII**

### **CONCLUSION AND RECOMMENDATIONS**

In this chapter, a summary of the entire work is first introduced, followed by conclusions and some recommendations to extend the current work in future.

#### **7.1 Summary**

An optimization problem for demand estimation in water networks was formulated, validated, and tested using three different case studies. The mathematical formulation was developed within a nonlinear programming framework. The mathematical programming language AMPL (Fourer et al 2003) was used to code the model and IPOPT (Wachter 2002) was selected as a solver. The problem was formulated using a standard least-squares objective with a regularization term based on historical data. To validate the model, the water network simulator EPANET was used first to simulate each case study and provide the flow and the pressure measurements. In the validation mode, the flows and pressures obtained from the simulator EPANET were compared to those obtained from the optimization formulation using full demand information. The estimation formulation was then tested using limited flow information from EPANET, as “online” measurements. The accuracy was evaluated by comparing the estimated flows and the corresponding flows from EPANET.

#### **7.2 Conclusion**

There are a number of potential uses for reliable online estimates of the water network demands. Many control and operations formulations, as well as security applications rely on estimates of the network flow velocities. This research has demonstrated that it is possible to estimate the unknown demands using a relatively sparse sensor network, even when these sensors are placed randomly. The work has also shown that offline demand estimates can be used to assist the online estimation

formulation. This regularization term forces a unique solution to the optimization problem. From the family of solutions that are able to satisfy the measurements, this formulation tends towards solutions that most closely match the historical estimates. This research demonstrates that this approach has merit, however, further investigation of appropriate regularization and updates are necessary.

### 7.3 Recommendations

Future studies that could advance the current work include the following:

- It was interesting to see that there were significant drops in the error with the addition of certain sensors. This implies that there may be optimal sensor layouts that consistently allow reasonable results with very few measurements. The error as a function of sensor layout needs to be studied in more detail and optimal strategies for layout should be investigated.
- In this work, the estimation considered flow measurements only. Future work should consider multiple sensor types and investigate the optimal allocation and layout of these sensors.
- This work considered relatively small networks ( $\sim 100$  nodes). Future work should also test the approach on larger networks. The largest of these problems was solved in less than one second, and we are confident that the solver can scale efficiently to larger networks. Of greater concern is the required number of sensors for these larger networks.
- Here, the assumed flows differed from the true flows by relative noise only, potentially biasing our results. Future work should investigate the effect of correlated errors should be investigated.

## REFERENCES

- Alperovits, E., and Shamir, U. (1977). "Design of optimal water distribution systems." *Water Resour. Res.*, 13(6), 885-90.
- Bang-Jensen, J., and Gutin, G. (2000). *Digraphs: Theory, Algorithms, and Applications*. Springer-Verlag. New York.
- Bhave, P. R. (2003). *Optimal Design of Water Distribution Networks*. Alpha Science International Ltd., Pangbourne, UK.
- Boccelli, D. L., Tryby, M. E., Uber, J. G., Rossman, L. A., Zierolf, M. L., and Polycarpou, M. M. (1998). "Optimal scheduling of booster disinfection in water distribution system." *J. Water Resour. Plan. Manage.*, 124(2), 99–111.
- Bondy, J. A., and Murty U. S. (1976). *Graph Theory with Applications*. The Macmillan Ltd., London, UK.
- Bull, R. J., and Kopfler, R. C. (1991). "Health effects of disinfectants and disinfection by Products." American Water Association Research Foundation, Denver, CO.
- Cesario, L. (1995). "Modeling, analysis, and design of water distribution systems." American Water Works Association, Denver, CO.
- Diestel, R. (2005). *Graph Theory*. Springer-Verlag. New York.
- Eiger, G., Shamir, U. and Ben-Tal, A. (1994). "Optimal design of water distribution networks." *Water Resour. Res.*, 30 (9), 2637–46.

- Fourer, R., Gay, M. D., and Kernighan, W. B. (2003). *AMPL a Modeling Language for Mathematical Programming*. Thomson TM, Waterbury, CT.
- Fujiwara, O., and De Silva, A. (1990). "Algorithm for reliability based optimal design of water networks." *Envir. Engrg.*, ASCE, 116(3), 575-587.
- Fujiwara, O., and Tung, H. (1991). "Reliability improvement for water distribution networks through increasing pipe size." *Water Resour. Res.*, 27(7), 1395-1402.
- Goulter, I. C. (1992). "Systems analysis in water-distribution network design: From theory to practice." *J. Civil Eng. Sys.*, 4(4), 175-84.
- Guan, J., Aral, M., Maslia, L. M., and Grayman, M. W. (2006). "Identification of contamination sources in water distribution systems using simulation-optimization method: Case study." *J. Water Resour. Plan. Manage.*, 132(4), 252-262.
- Islam, M. R., Chaudhary, M. H., and Clark, R. M. (1997). "Inverse modeling of chlorine concentration in pipe networks under dynamic condition." *J. Envir. Eng.*, 123(10), 1033-1040.
- Kaplelan, Z. S., Savic, D. A., and Walters, G. A. (2005) "Multi-objective design of water distribution system under uncertainty." *J. Water Resour. Resr.*, 41, 67-77.
- Kizilenis G. (2006) "Optimal sensor locations in water distribution in water distribution networks." M.S. thesis, Sabanci University, Istanbul, Turkey.
- Laird, C. D., Biegler, L. T., Bloemen Waanders, B. G., and Bartlet, R. A. (2005). "Contamination source determination for water networks." *J. Water Resour. Plan. Manage.*, 131 (2), 125-134.



- Laird, C. D., Biegler, L. T., and van Bloemen Waanders, B. G. (2006). "Mixed-integer approach for obtaining unique solutions in source inversion of water networks." *J. Water Resour. Plann. Manage.*, 132(4), 242–251.
- Morgan, D., and Goulter, I. (1985). "Optimal urban water distribution design." *Water Resour. Res.*, 21(5), 642-652.
- Ostfeld, A., and Salomons, E. (2004). "Optimal operation of multiquality water distribution systems: Unsteady conditions." *Engrg. Optimization*, 36(3), 337-359.
- Quindry, G., Brill, E., and Liebman, J. (1981). "Optimization of looped water distribution systems." *J. Envir. Engrg. Div.*, ASCE, 107(4), 665-679.
- Rahal, H. (1995). "A co-tree flows formulation for steady state in water distribution networks." *Adv. Eng. Software*, 22(1995) 169-178.
- Rossmann, L. A., Clark, R. M., and Grayman, W. M. (1994). "Modeling chlorine residuals in drinking water distribution systems." *J. Envir. Eng.*, 120(4), 803–817.
- Rossmann, L. A. (2000). *EPANET 2 users manual*, National Risk Management Research Laboratory, U.S. EPA, Cincinnati, Ohio
- Savic, D. and Walters, G. (1997) "Genetic algorithms for least cost design of water distribution network." *J. Water Resour. Plang. and Mgmt.*, ASCE, 123(2), 67–77.
- Shang, F., Uber, J., and Polycarpou, M. (2002). "Particle backtracking algorithm for water distribution system analysis." *J. Envi. Eng.*, 128(5), 441–450.

- Shang, F., Uber, J., Waanders, B., Boccelli, D., and Janke, R. (2006). "Real time water demand estimation in water distribution systems." *8th Annual Water Distribution System Analysis Symposium*, Cincinnati, Ohio, 1-14.
- Sharp, W. W., Pfeffer, J., and Morgan, M. (1991). "In-situ chlorine decay rate testing." *Proc., Water Quality Modeling in Distribution Systems Conf.*, AWWA Research Foundation, Denver, Colo.
- Vairavamoorthy, K., and Ali, M. (2000). "Optimal design of water distribution systems using genetic algorithms" *Computer-Aided Civil and Infrastructure Engineering.*, 15, 374-382.
- Varma, K. V., Narasimhan, S., and Bhallamudi S. M. (1997). "Optimal design of water distribution system using a NLP method." *J. Envir. Engrg.*, 123(4), 381-388.
- Wable, O., Dumoutier, N., Duguet, J. P., Jarrige, P. A., Gelas, G., and Depierre, J. F. (1991). "Modeling chlorine concentrations in a network and applications to Paris distribution network." *Proc., Water Quality Modeling in Distribution Systems Conf.*, AWWA Research Foundation, Denver, Colo.
- Wachter, A. (2002). "An interior point algorithm for large-scale nonlinear optimization with applications in process engineering." PhD thesis, Carnegie Mellon Univ., Pittsburgh, PA.
- Walski, T. M., Gessler, J., and Sjostrom, J. (1990). *Water Distribution Systems: Simulation and Sizing*. Lewis Publishers, Chelsea, MI.
- Walski, T. M., Chase, D. V., and Savic, D. A. (2001). *Water distribution Modeling*. Haestad Press, Waterbury, CT.

Wood, D. J., and Funk, J. E. (1993). "Hydraulic analysis of water distribution systems." E. Cabrera and F. Martinez, eds., *Water Supply Systems, State of the Art and Future Trends*, Computational Mechanics Publications, Southampton, UK, 41-85.

Zierolf, M., Polycarpou, M., and Uber, J. (1998). "Development and autocalibration of an input-output model of chlorine transport in drinking water distribution systems." *IEEE Trans. Control Syst. Technol.*, 6(4), 543–553.

## APPENDIX A

This appendix describes the optimization formulation which was coded using the programming language AMPL. Case Study 1 is selected to show example of the optimization formulation. There are almost no differences between the three mathematical models that describe the three case studies with very few exceptions when no-tank or no-reservoir statement is added to the model or when specific method for labeling the nodes and the links is required to match exactly the corresponding labeling in EPANET. The first section in this appendix describes the AMPL code, while the second section show example of the input data file.

A-1: AMPL code for Case Study 1:

### # Network Structure

```

## Nodes:
set Nodes;

param CN { Nodes } default 1;           # defines nodes not tanks
param CT { Nodes } default 0;           # 1 if only node i is a tank
param DT { i in Nodes : CT[i]=1 } ;    # Diameter of tank i
param AT { i in Nodes : CT[i]=1 } := (3.141592654/4) * (DT[i]^2);
param hoT { i in Nodes: CT[i]=1 } ;    # initial height in tank i

## Pipes:
set Links;
set Chords within Links;
set Measurements;

param SM;
param EM;
set MeasurementsLables: = SM .. EM;
set Numberofmeasurements;

```

```

param idx {MeasurementsLables};
param CIN { k in Links };           # Index of Inlet Node to Link K
param COU { k in Links };           # Index of outlet Node to Link K

# Unsteady state
param ST;
param ET;
set Times ordered := ST..ET;
param t { j in Times union {ET+1}};
param DMPG { j in Times };
param DMP15 { j in Times };
param DMP35 { j in Times };
param DMP123 { j in Times };
param DMP203 { j in Times };
param FIMP { i in Nodes, j in Times } default 0;

# Material Balance
param CR { Nodes } default 0;       # identifies a reserviour at Node i
param FI { Nodes } default 0;       # The known inlet flow at node i
param Sd { Nodes } ;                # Identifies the data of the measured demands
param dd { j in Times } >=0;
param STD { j in Times };

# Hydraulics
param Z { Nodes } ;                 # The elevation at each Node
param L { Links } >= 0;              # The Length of each Pipe
param D { Links } >= 0;              # The diameter of each Pipe
param Cpump { Links } default 0;    # 1 if thers is a pump between Nodes at time j

```

```

param CSP { k in Links, j in Times : Cpump[k]=1 } default 1;
param CSL { k in Links, j in Times : Cpump[k]=0 } default 1;
param A { k in Links : Cpump[k]=1 };           # 1 st parameter in Pump Equation
param B { k in Links : Cpump[k]=1 };           # 2 nd parameter in Pump Equation
param n { k in Links : Cpump[k]=1 };

```

```

## Hazen williams Eqn:

```

```

param C;
param b;                                     # The power in the formula
param a {k in Links } := (4.727) * C[k]^(-1.852)* ((D[k]/12)^(-4.871)) * L[k];

```

### # Optimization

```

param CF {k in Links } default 0;
param SF {k in Links, j in Times } ;
param WF;
param Wd;

```

### # variables

```

var H { Nodes, Times } :=20;
var d { Nodes, Times } :=2.0;               # The demands at Nodes
var Diffd { i in Nodes, j in Times } = d[i,j] - DMPG[j]*Sd[i];
var weightederror { i in Nodes, j in Times } = if (Sd[i]=0) then 0 else if (Sd[i]!=0)
                                                then (100*abs(Diffd[i,j])/abs(Sd[i]));
var avweightederror { i in Nodes } = sum { j in Times } weightederrord[i,j]/ ET;
var ovsumweightederror = sum {i in Nodes} avweightederrord[i]/96;

var P { i in Nodes, j in Times } = 0.43330003404 * H[i,j];
var DiffP { i in Nodes, j in Times } = P[i,j] - SP[i,j];

```

```

var weightederrorP {i in Nodes, j in Times} = if (SP[i,j]=0) then 0 else
(100*abs(DiffP[i,j])/abs(SP[i,j]));
var avweightederrorP { i in Nodes } = sum {j in Times} weightederrorP[i,j]/ 25;
var ovsumweightederrorP = sum{i in Nodes} avweightederrorP[i]/96;

var FR { i in Nodes, Times : CR[i]=1 } :=1.0;      # The inlet Flows to the Network from
reservoirs at time j
var F { k in Links, j in Times } := 1.0;
var DiffF { k in Links, j in Times } = F[k,j] - SF[k,j];
var weightederrorF {k in Links, j in Times} = if (SF[k,j]=0) then 0 else (100*
abs(DiffF[k,j])/abs(SF[k,j]));
var avweightederrorF { k in Links} = sum {j in Times} weightederrorF[k,j]/ET;
var ovsumweightederrorF = sum{k in Links} avweightederrorF[k]/117;

var ACCT { i in Nodes, j in Times: CT[i]=1 } := 1.0; # accumulation term in the tanks
var hp { k in Links, j in Times : Cpump[k] = 1 } = (A[k] - B[k]*(abs(F[k,j]))^n[k]);
var hL { k in Links, j in Times : Cpump[k] = 0 } = a[k] * (abs(F[k,j]*0.1336660135/60))^b;
var LevelT { i in Nodes, j in Times union {ET+1} :CT[i]=1 } := 1.0;
var THT { i in Nodes, j in Times union {ET+1} : CT[i]=1 } = LevelT[i,j] + Z[i];
var RY { k in Links, j in Times } = (3162.2)*(abs(F[k,j])/D[k]);
var RYL { k in Links, j in Times } = if ( RY[k,j] < 2000) then RY[k,j] else 0;
var RYtr { k in Links, j in Times } = if ( RY[k,j] >= 2000) then if (RY[k,j]< 4000) then RY[k,j]
else 0;
var RYT { k in Links, j in Times } = if ( RY[k,j] >= 4000) then RY[k,j] else 0;

# Objective Function
minimize objfn : Wd * sum { i in Nodes, j in Times } ((d[i,j] - (DMPG[j]*Sd[i]*dd[j]))^2)+

```

$$WF * \sum \{ k \text{ in Links}, j \text{ in Times} : CF[k]=1 \} ((F[k,j] - SF[k,j])^2);$$

### # Constraints

$$\text{subject to limit\_MBN} \{ i \text{ in Nodes}, j \text{ in Times} : CN[i]=1 \}:$$

$$(FIMP[i,j]*FI[i] + \sum \{ k \text{ in Links}: COU[k]=i \} (F[k,j]) - \sum \{ k \text{ in Links}: CIN[k]=i \} (F[k,j]) - d[i,j]) = 0;$$

$$\text{subject to limit\_MBR} \{ i \text{ in Nodes}, j \text{ in Times} : CR[i]=1 \}:$$

$$(FR[i,j] + \sum \{ k \text{ in Links}: COU[k]=i \} (F[k,j]) - \sum \{ k \text{ in Links}: CIN[k]=i \} (F[k,j])) = 0;$$

$$\text{subject to limit\_MBT} \{ i \text{ in Nodes}, j \text{ in Times} : CT[i]=1 \}:$$

$$(\sum \{ k \text{ in Links}: COU[k]=i \} (F[k,j]) - \sum \{ k \text{ in Links}: CIN[k]=i \} (F[k,j]) - ACCT[i,j]) = 0;$$

$$\text{subject to limit\_ReservoirHead} \{ i \text{ in Nodes}, j \text{ in Times}: CR[i] = 1 \} : H[i,j] = 0;$$

$$\text{subject to limit\_TL} \{ i \text{ in Nodes}, j \text{ in Times}: CT[i]=1 \}:$$

$$(LevelT[i,j+1] - LevelT[i,j] - (t[j+1]-t[j]) * (0.1336660135/AT[i])* ACCT[i,j]) = 0;$$

$$\text{subject to limit\_TH} \{ i \text{ in Nodes}, j \text{ in Times}: CT[i]=1 \}:$$

$$LevelT[i,j] = H[i,j] ;$$

$$\text{subject to limit\_IHT} \{ i \text{ in Nodes}: CT[i]=1 \}:$$

$$H[i,0] = hoT[i];$$

$$\text{subject to limit\_hydraulicLO} \{ k \text{ in Links}, j \text{ in Times}: Cpump[k]=0 \text{ and } CSL[k,j]=1 \}:$$

$$(H[CIN[k],j] + Z[CIN[k]] - H[COU[k],j] - Z[COU[k]] + (\text{if } (F[k,j]) \geq 0 \text{ then } - hL[k,j] \text{ else } + hL[k,j])) = 0;$$



subject to limit\_hydraulicLC { k in Links, j in Times: Cpump[k]=0 and CSL[k,j]=0 }:

$$F[k,j] = 0 ;$$

subject to limit\_hydraulicPO { k in Links, j in Times: Cpump[k]=1 and CSP[k,j]=1 }:

$$(H[CIN[k],j] + Z[CIN[k]] + hp[k,j] - H[COU[k],j] - Z[COU[k]]) = 0 ;$$

subject to limit\_hydraulicPC { k in Links, j in Times: Cpump[k]=1 and CSP[k,j]=0 }:

$$F[k,j] = 0 ;$$

subject to limit\_Zerodemand { i in Nodes, j in Times: CT[i]=1 or CR[i]=1 }:

$$d[i,j] = 0 ;$$

A-2: AMPL data input file:

```

#Network structure:
set Nodes := 2,9,10,11,12,13,21,22,23,31,32;
set Links := 9,10,11,12,21,22,31,110,111,112,113,121,122;
set Chords := 12,111, 122;
set Measurements:= 9 31 110 113 10 112 121 22 11 21;
param SM:=1;
param EM:=10;
param: idx:=
1 9
2 31
3 110
4 113
5 10
6 112
7 121
8 22
9 11
10 21;
#Time frame:
param ST:=0;
param ET: =24;
param:
t :=
0 0
1 60
2 120
3 180

```

4	240
5	300
6	360
7	420
8	480
9	540
10	600
11	660
12	720
13	780
14	840
15	900
16	960
17	1020
18	1080
19	1140
20	1200
21	1260
22	1320
23	1380
24	1440
25 6	1500;

param:

DMPG :=

0	1
1	1
2	1.2
3	1.2
4	1.4
5	1.4
6	1.6
7	1.6
8	1.4
9	1.4
10	1.2
11	1.2
12	1.0
13	1.0
14	0.8
15	0.8
16	0.6
17	0.6
18	0.4
19	0.4
20	0.6
21	0.6
22	0.8
23	0.8
24	1.0;

param Wd := 0.01;  
 param WF := 1.000;

#Nodes Data:

param:

	Z	Sd:=
10	710	0
11	710	150
12	700	150
13	695	100
21	700	150
22	695	200
23	690	150
31	700	100
32	710	100
9	800	0
2	850	0;

#Links Data:

param:	CIN	COU	L	D :=
10	10	11	10530	18
11	11	12	5280	14
12	12	13	5280	10
21	21	22	5280	10
22	22	23	5280	12
31	31	32	5280	6
110	2	12	200	18
111	11	21	5280	10

112	12	22	5280	12
113	13	23	5280	8
121	21	31	5280	8
122	22	32	5280	6
9	9	10	0	12;

# Hydraulics:

## Friction Model:

### Hazen Williams:

param b:= 1.852;

param C:= 100;

#param C:= 120;

#let commands:

##Tanks

let CN[2] := 0;

let CT[2] := 1;

let DT[2] := 50.5;

let hoT[2]:= 120;

## (CR[i] = 1),for reservoir

let CR[9] := 1;

let CN[9] := 0;

##Pumps

let Cpump[9]:=1;

##Pump parameters:

let A[9]:=333.333;

```
let B[9]:=0.00003704;
let n[9]:=2;

let CSP[9,13]:=0;
let CSP[9,14]:=0;
let CSP[9,15]:=0;
let CSP[9,16]:=0;
let CSP[9,17]:=0;
let CSP[9,18]:=0;
let CSP[9,19]:=0;
let CSP[9,20]:=0;
let CSP[9,21]:=0;
let CSP[9,22]:=0;

for {j in Times}
{
let STD[j]:= 0.1;
let dd[j]:= abs( Normal(1,STD[j]) );
}
```

## VITA

Name: Ahmed Ibrahim Elsaid Rabie

Address: Department of Chemical Engineering  
c/o Dr. Carl Laird  
TAMU  
College Station, TX, 77843-3122

Email Address: arabie2310@gmail.com

Education: B.Sc., Chemical Engineering, Cairo University, 2001  
M.Sc., Chemical Engineering, Cairo University, 2006  
M.Sc., Chemical Engineering, Texas A&M University, 2008